Unprecedented thiacalixarene fucoclusters strong inhibitors of Ebola cis-cell infection and HCMV-gB glycoprotein/DC-SIGN C-type lectin interaction

Marwa Taouai,[†,§,£] Vanessa Porkolab,[††,£] Khouloud Chakroun,[†,§,£] Coraline Cheneau,[‡,£] Joanna Luczkowiak,[¥,£] Rym Abidi,[§] David Lesur,[†] Peter J. Cragg,[π] Franck Halary,[‡] Rafael Delgado,[¥] Franck Fieschi, [††*] Mohammed Benazza[†*]

[†]Laboratoire de Glycochimie des Antimicrobiens et des Agroressources (LG2A-UMR7378-CNRS), Université de Picardie Jules Verne, 10 Rue Baudelocque, 80039, Amiens Cédex, France. E-mail: mohammed.benazza@u-picardie.fr.

[§]Faculté des Sciences de Bizerte, Laboratoire d'Application de la Chimie aux Ressources et Substances Naturelles et à l'Environnement (LACReSNE) Unité «Interactions Moléculaires Spécifiques», Université de Carthage Zarzouna-Bizerte, TN 7021, Tunisia.

[††]Univ. Grenoble Alpes, CNRS, CEA, Institut de Biologie Structurale, F-38044 Grenoble, France. E-mail: franck.fieschi@ibs.fr

[‡]1. Centre de Recherche en Transplantation et Immunologie (ou CRTI) UMR 1064, Inserm, Université de Nantes, Nantes, France; 2. Institut de Transplantation Urologie Néphrologie (ou ITUN), CHU Nantes, Nantes, France

[¥]Laboratorio de Microbiología Molecular, Instituto de Investigación Hospital 12 de Octubre (imas12), Madrid 28041, Spain

[π] School of Pharmacy and Biomolecular Science, University of Brighton, Brighton BN2 4GJ, UK.

KEYWORDS. *Ebola virus, EBOV, HCMV, DC-SIGN, Thiacalixarene, Calixarene, Ugi-4CR.*

ABSTRACT: Glycan–protein interactions control numerous biological events from cell-cell recognition and signaling to pathogen host cell attachment for infections. To infect cells, some viruses bind to immune cells thanks to DC-SIGN (dendritic cell [DC]-specific ICAM3-grabbing non-integrin) C-type lectin expressed on dendritic and macrophage cell membrane, via their envelope protein. Prevention of this infectious interaction is a serious therapeutic option. Here, we describe the synthesis of first water-soluble tetravalent fucocluster pseudopeptide-based thiacalixarene 1,3-alternate as viral antigen mimics designed for the inhibition of DC-SIGN, to prevent viral particle uptake. Their preparation exploits straightforward convergent strategies involving one pot Ugi four-component (Ugi-4CR) and azido-alkyne click chemistry reactions as key steps. Surface plasmon resonance showed strong inhibition of DC-SIGN interaction properties by tetravalent ligands designed with high relative potencies and β avidity factors. All ligands block DC-SIGN active sites at nanomolar IC_{50} preventing cis-cell infection by Ebola viral particles pseudotyped with EBOV glycoprotein (Zaïre species of Ebola virus) on Jurkat cells that express DC-SIGN. In addition, we observed strong inhibition of DC-SIGN/human cytomegalovirus (HCMV)-gB recombinant glycoprotein interaction. This finding opens the way to the simple development of new models of water-soluble glycocluster-based thia-calixarene with wide-range antimicrobial activities.

INTRODUCTION

The ability of viruses to resist traditional drugs is a crucial problem in current antiviral therapy.[1,2] The widely approved antiviral drugs act intracellularly. Unfortunately, their toxicity and the rapid mutation of viruses lie behind the development of viral drug-resistance, strongly decreases therapeutic relevance.[3] This dramatic crisis in health control is exacerbated by severe co-infections by different germs in immunocompromised patients (e.g. *Mycobacterium*/HIV-1,[4] HCMV/HIV-1,[5] etc.). Consequently, the design and straightforward access to novel efficient drugs with a broad spectrum of antimicrobial action regardless of the pathogen's structural nature or resistance range, is urgently required. It is possible to develop such drugs by targeting the neutralization of common extracellular infectious mechanisms such

as glycan-protein interactions.[6,7] Viruses (e.g. HIV-1,[8] HCMV,[9] Ebola,[10] SARS coronavirus, dengue[11]), along with some bacteria and parasites (e.g. *Mycobacterium*,[12] *Leishmania*[13]), use this kind of interaction for their attachment to host cells, a preliminary step for their uptake with the view of subverting intracellular biosynthetic processes to their replication.[14] Typically, the tetrameric transmembrane DC-SIGN C-type-lectin (dendritic cell [DC]-specific ICAM3-grabbing non-integrin) that is expressed at innate immune system macrophage and DC membranes, serves as a key receptor for viral antigen-containing carbohydrates (e.g. DC-SIGN/viral glycoproteins such as HIV-1-gp120, HCMV-gB, Ebola-GP etc.).[6,7,14,15] It is a key target that has stimulate the design of inhibitors as new tools to overcome attachment of pathogen to host cells to hinder the infectious process. Inspired by some effective monomeric inhibitors of enzymes (e.g. Glycosidases, glycosyltransferases etc.),[16, 17,18,19] small non-carbohydrate molecules as μ-molar IC_{50} inhibitors of DC-SIGN have emerged (e.g. Quinoxalinone inhibitors…).[20,21] Glycomimetics compounds, mimicking natural ligand but having better stability, represent also popular alternative extensively explored now to target C-type lectin.[22,23,24] As wide range of lectins,[25,26] DC-SIGN is a multimeric protein naturally endowed with moderate affinity for specific monovalent sugars (e.g. only millimolar IC_{50} inhibition with L-fucose).[27,28] However, suitable multipresentation of sugars create synergistic multiple binding events that enhance the avidity (apparent affinity).[28,29] Thus, the use of multivalent viral glycan mimics to target DC-SIGN is a virustatic option that has triggered the design and assessment of a large panel of potentially relevant multivalent scaffolds such as mannosylated polymers,[30] proteins,[31] peptides,[32] dendrimers,[33,34,28] gold nanoparticles,[35] fullerene,[36] and recently, carbon nanotube hybridized fullerene.[37] The models designed strongly inhibit DC-SIGN but their development often uses uncommon and sophisticated building blocks that are difficult to handle. *p*-tBu-thiacalixarene is one of the cheapest platforms used for many applications including the detection and separation of biologically important ions, and the synthesis of self-assembled coordination cages or multinuclear complexes.[38] However, this molecule is under-exploited in the multivalent glycocluster field, despite its availability and simple transformation.[39] Here, we describe the first method for straightforward synthesis of fucocluster **1** and **2** based on *p*-tBu-thiacalixarene 1,3-alternate (Figure 1A). We rationalized

their design following data in the literature related to the structure of DC-SIGN, the preference basis of L-fucose rather than that of the widely used D-mannose epitope, and water-solubility. The last point is particularly important as it represents a challenging problem when thiacalixarene and their congeners are used as scaffolds. First, we assessed both fucoclusters **1** and **2** as DC-SIGN inhibitors by surface plasmon resonance (SPR) technology using BSA-mannotriose functionalized surface (BSA-manα1-3[manα1-6]man). Such surface allows addressing DC-SIGN/polymannose surface interaction and is a mimic of the DC-SIGN binding to HIV-1-gp120, which harbor high mannose glycans. Then, we evaluated binding inhibition of DC-SIGN/HCMV gB recombinant glycoproteins. Finally we assessed both ligands with respect to DC-SIGN-dependent host cell entry and infection by experimental Ebola virus viral particles pseudotyped with the recently emerged Zaïre species (EBOV). For impact evaluation of the scaffold topology, we synthesized and similarly assessed *p*-tBu-calix[4]arene fucocluster **3,** which has a cone conformation (Figure 1B).

RESULTS AND DISCUSSION

Rationalized design and synthesis of glycoclusters 1, 2 and 3. Like its calixarene congener,[40] thiacalixarene is highly hydrophobic.[41] This compromises biological assessment in aqueous media.[42] Using calixarene analogues, this problem could be solved when a glycoconjugated alkyl spacer was linked to *p*-tBu-calix[4]arene via a peptide moiety.[43] Consequently, we targeted glycoconjugate **1** and **2** based *p*-tBu-thiacalix[4]arene 1,3-alternate linked to a pseudopeptide-bearing spacer (Figure 1). The four pseudopeptide sequences and the four fucose units should be synergistically favorable to the water-solubility of glycocluster **1**, and largely to that of glycocluster **2**, due to the hydrophilic glycylglycylhydroxamic acid groups. As for iron chelation, the hydroxamic acid groups could also play a role in iron depletion, as another therapeutic attack strategy, against iron-dependent microbes.[44] In contrast, DC-SIGN have affinity for D-mannose and L-fucose in a Ca^{2+}-dependent multivalent fashion, and both sugars could be considered natural epitope of DC-SIGN. Two adjacent sites of the four carbohydrate recognition domains (CRDs) of DC-SIGN arranged on a single face are separated by about

38 to 40 Å, whereas opposite sites lie about 61 Å apart (Figure 2A).[45] Following the interactions of L-fucose in fucosylated glycans, and mannose in high mannose with DC-SIGN, the predominant binding could be chelation and/or statistical binding rebinding. This ensure a high density of sugars around CRDs. Hydroxyl groups in position 3 and 4 of L-fucose or D-mannose are the main contributor to binding interactions,[8] which probably explains non-selective L-fucose and D-mannose recognition. To avoid, or at least diminish, the inhibition of some mannose specific lectins, such as langerin,[46] involved in the vaginal mucosa in the defense against HIV-1 infection, we decided to investigate L-fucose. Without a cooperative effect of other neighboring sugars in heteroglycocluster systems, langerin only recognizes this sugar inefficiently. Other mannophilic lectins of the innate defense system, such as the mannose binding lectin (MBL),[47] could also be saved from inappropriate inhibition. Further reasons to advocate L-fucose use include its possible synergistic involvement as a carbohydrate-specific signaling molecule through specific binding to DC-SIGN. This provides action against invading pathogens via the initiation of T-helper cell differentiation.[48] Finally, the length of the spacer arm was rationalized via molecular mechanic (MMFF) prediction of the greatest possible separation between two fucose units (See SI, Figure S31). We stated that approximately 50 to 55 Å should be enough to cover the highest distance of about 40 Å between two adjacent CRDs by folding, in the event of the chelation mechanism.[45] Furthermore, fucoclusters **1** and **2** could be considered an assembly of two bivalent systems separated by a rigid core (Thiacalixarene). This echoes other reported rigid multivalent glycoclusters (e.g. the rods of Bernardi et al[49]). Both ligands also have the possibility of addressing two directional binding approaches toward DC-SIGN (Figure 2B), which should be favorable statistically for efficient interaction with DC-SIGN. Taking into account all these structural considerations, we targeted cooperative effects to increase the strength of binding to DC-SIGN of the ligands we examined.

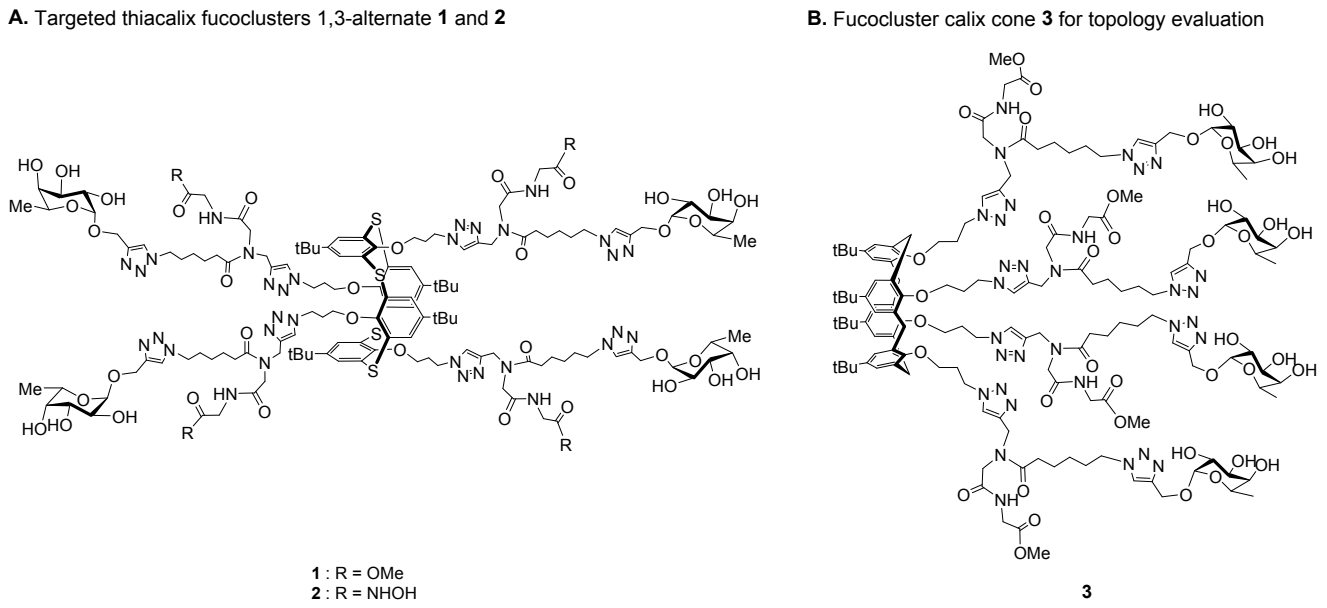

Figure 1. New designed fucoclusters **1**, **2** and **3** for inhibition of DC-SIGN dependent viral infections.

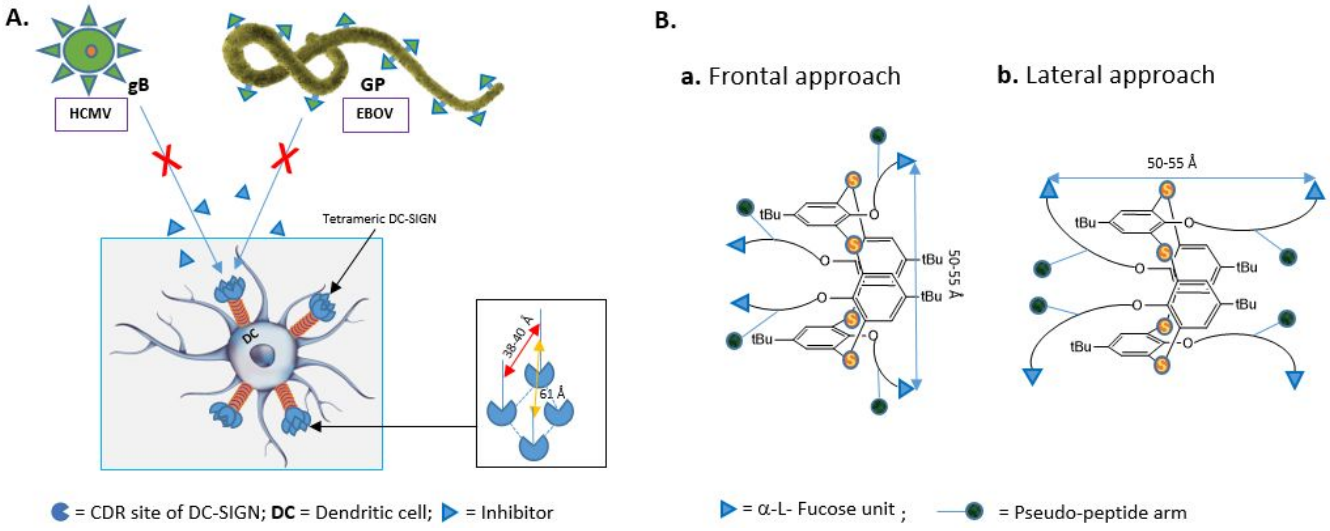

Figure 2. A. Distances between CRDs in DC-SIGN; **B**. Binding approaches to DC-SIGN of thiacalixarene fucoclusters **1** and **2;** Distances between two fucose units were estimated via molecular mechanic (MMFF) prediction (See SI, Figure S31).

We synthesized fucocluster **1** and its tetrahydroxamic acid derivative **2** following the convergent strategy described in scheme 1. For the multivalent presentation of L-fucoside moieties, we used the previously described tetrachloroalkyloxy-*p*-tBu-thiacalixarene 1,3-alternate **5** that is readily obtained in 93 % yield from the commercially available cone conformation of *p*-tBu-thiacalix[4]arene **4** (path 1).[50] The

conventional azidation of molecule **5** gives the tetra-alkoxyazido-*p*-tBu-thiacalix[4]arene derivative **6** (in 94% yield) as the sugar acceptor. This can easily be transformed into a glycoconjugate via a click chemistry reaction.[39] To tailor the required distance between two sugars in an elongated conformation, we used a coupling association of propargyl amine and the commercially available 6-bromo-hexanoic acid obtained via the Ugi four-component reaction (Ugi-4CR). Following pathway 2, the one pot Ugi-4CR took place in methanol at room temperature by mixing together amine and paraformaldehyde to form an imine intermediate. This reacts subsequently with bromo-carboxylic acid and isocyanatoacetate to give the propargyl-glycylglycinate derivative **7** in 67% yield following a well-known mechanism.[51] The latter was fully characterized to be a mixture of rotamers identified by ^{13}C NMR spectroscopy using three pairs of signals that are representative of carbonyl groups in a ratio of about 1/0.5 at 173.59/173.22, 170.05/169.89 and 169.07/168.53 ppm.

The subsequent click chemistry of the tetraazido-thiacalixarene **6** with the Ugi adduct **7** was carried out successfully under $CuSO_4.5H_2O$/Na-ascorbate with a mixture of THF/MeOH/tBuOH under conventional heating, to give tetrabrominated glycylglycinate thiacalixarene **8**. Due to the four glycylglycinate peptide moieties, this hybridized thiacalixarene seemed to demonstrate a strong interaction with acidic silica gel for migration. Consequently, neutralization with 1% NEt_3 as the base was necessary to separate molecule **8** in a 58% yield using an acetone/ethylacetate/cyclohexane mixture as the eluent. Subsequent azidation under conventional conditions (NaN_3, DMF, 90 °C) gave an excellent yield (92%) of the tetrazido pseudopeptide derivative **9**. To obtain the desired compound, we tried two pathways: firstly, we gathered the known per-O-acetylated-1-O-propargyl-α-L-fucoside **10** and the tetraazidothiacalixarene **9** under click chemistry conditions using $CuSO_4.5H_2O$/Na-ascorbate in a mixture of THF/H_2O/tBuOH under conventional heating or using CuI/DIEA in acetonitrile under heating by microwaves. The last conditions are the preferred ones, since the reaction was rapid and gave a clean crude product containing fucoconjugate **11** as the main compound. This was separated in good isolated yield (62%), upon chromatography on neutralized silica gel. This *fuco*-tetramer is well-characterized by MS-ESI (m/z =

1853.1 $[M+2Na]^{2+}$) and NMR spectroscopy. The ^{13}C NMR spectroscopy for instance shows as main feature, the existence of rotamers, a consequence of conformational equilibrium that is widely encountered in peptoïde derivatives.[52] This behavior has no magnetic impact on fucose carbon atoms, whose signals are all represented by a single peak in the ^{13}C-spectrum. This facilitates their analysis (See SI, Figure S9). Unfortunately, a subsequent acetolysis reaction gave an unexpected mixture. This negative result arose from the second alternative reaction that uses the free *O*-propargyl α-L-fucoside **12** in the click chemistry step. Using CuI/DIEA in acetonitrile under microwave heat for 30 min, we obtained the targeted glycocluster **1** at a yield of 53 % from C18-reverse-phase chromatography with a suitable H_2O/CH_3CN eluent gradient. To transform the attached ester functions into hydroxamic acid groups that are more favorable to solubility in water, we reacted cluster **1** with a large excess of aqueous hydroxylamine and a catalytic amount of potassium cyanide in methanol, at room temperature. The cluster **2**, which derived from this was easily obtained at a yield of 54% after C18-reverse-phase chromatography with an H_2O/CH_3CN eluent gradient. Both compounds were characterized by NMR (See SI) and LC-MS that shows high purities and respective parent ions at m/z = 1578.98 $[M+2H]^{2+}$ and m/z =1053.39 $[M+3H]^{3+}$ for molecule **1**, and m/z = 1581.52 $[M+2H]^{2+}$ and m/z = 1054.45 $[M+3H]^{3+}$ for molecule **2** (See SI, Figures 25-28).

To evaluate the topological impact on DC-SIGN inhibition, we subsequently synthesized *p*-tBu-calix[4]arene fucocluster **3** using the same strategy (Schema 2). We started with the well-known cone conformation of tetraazido-propyloxy-*p*-tBu-calix[4]arene **13**[53] and the click chemistry reaction with Ugi-adduct **7**. We obtained tetrabromoalkyl-pseudopolypeptide **14** at a yield of 57%. Subsequent azidation gave the tethered azidoalkylpolypseudopeptide **15** in an almost quantitative amount. After click chemistry with propargyl fucoside **12**, the latter gave the expected fucocluster **3** at a yield of 49%. The structure of **3** was fully characterized by LC-MS using two parent ions at m/z = 1542.61 $[M+2H]^{2+}$ and m/z = 1028.92 $[M+3H]^{3+}$ (See SI, Figures 29-30), and in ^1H-NMR the cone conformation was characterized by the AB system of bridged $ArCH_2Ar$. This gave two doublet signals at 3.15 and 4.32 ppm with a J_{AB} coupling

constant of about 12 Hz. As expected, all three glycocluster-based thiacalixarene and calixarenes **1**, **2** and **3** obtained respectively in overall yields of 25% (5 steps), 13% (6 steps) and 15% (5 steps), are highly water soluble, which allows their biological assessment in aqueous media.

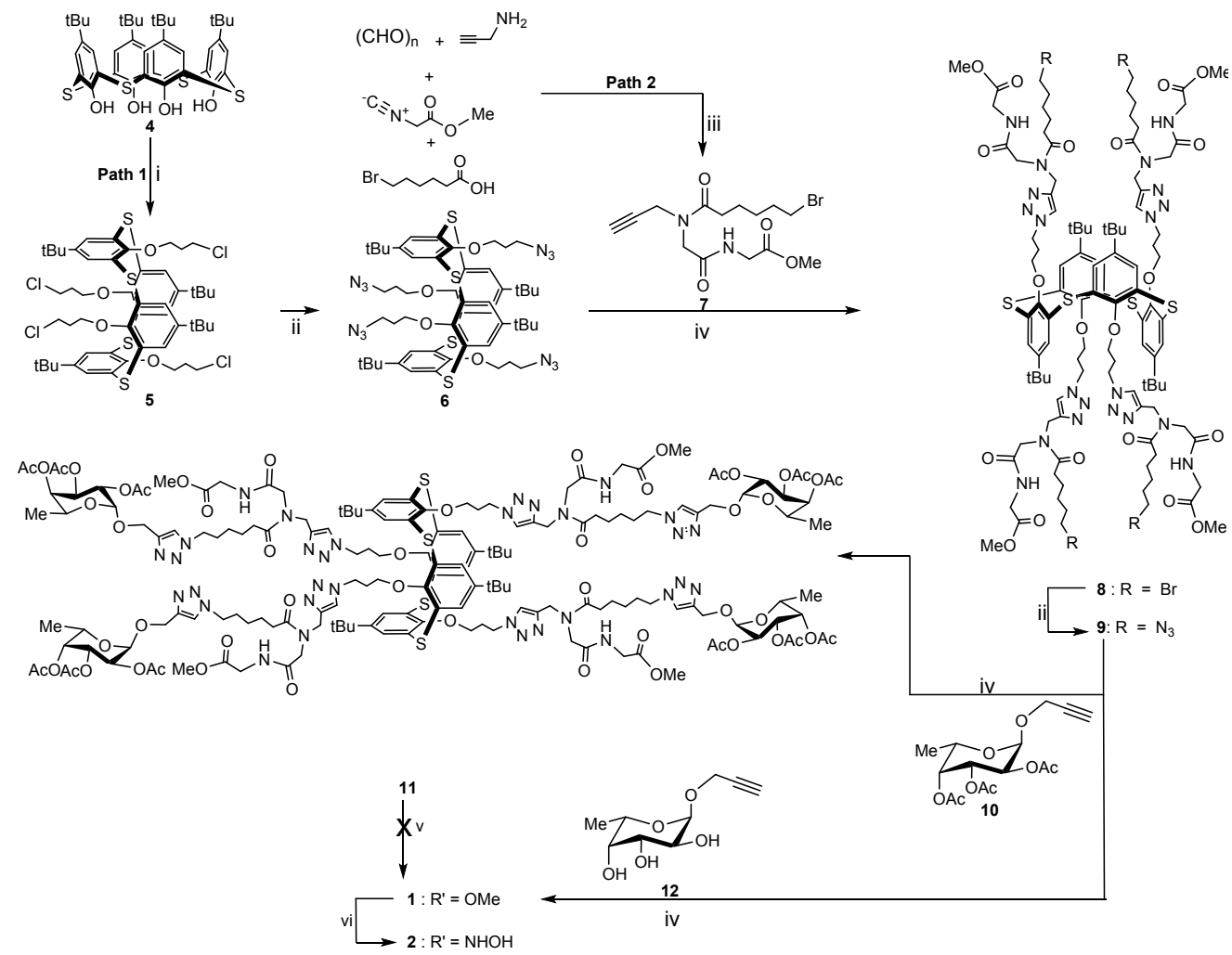

Scheme 1. Convergent strategy for synthesis of fucoclusters **1** and **2** using two key component, the Ugi adduct **7** and the tetraazido-thiacalixarene **6**. i. 1-Bromo-3-chloro-propane, K_2CO_3, refluxed acetone; ii. NaN_3, DMF, 90 °C; iii. MeOH, rt, 24h; iv. $CuSO_4.5H_2O$/Na-ascorbate, H_2O/THF/tBuOH, 60 °C, 3h, or CuI/DIEA, CH_3CN, MW, 30 min; v. MeONa, MeOH, rt; vi. NH_2OHaq, KCN_{cat}, MeOH/THF, rt.

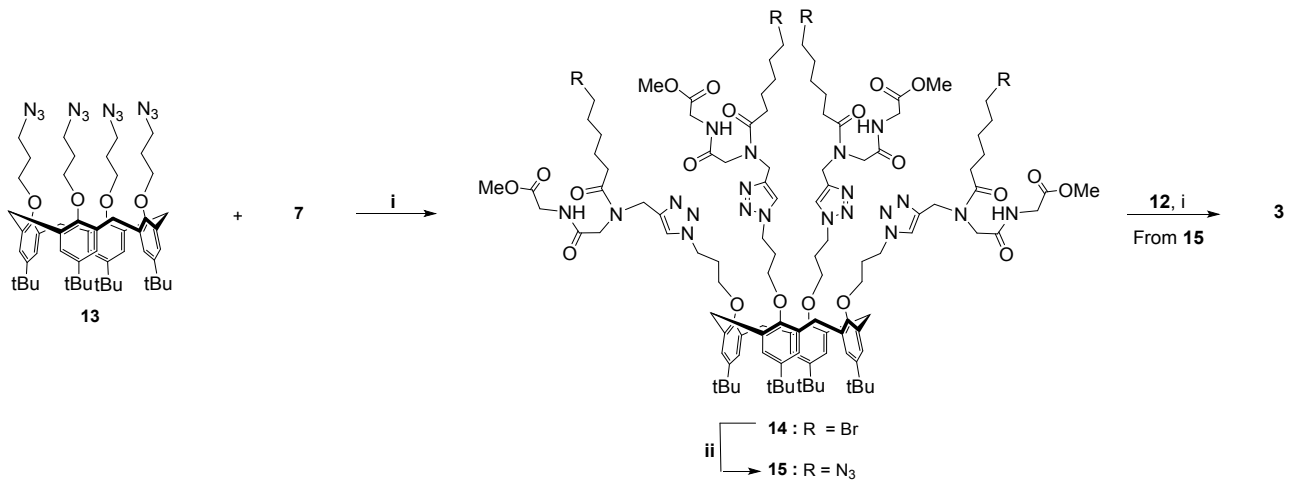

Schema 2. Synthesis of *p*-tBu-calix[4]arene fucocluster **3** via click-chemistry of UGI adduct **7** and tetraazidopropyloxy-*p*-tBu-calix[4]arene **13**. i. $CuSO_4.5H_2O$/Na-ascorbate, H_2O/THF/tBuOH, 60 °C, 3h, or CuI/DIEA, CH_3CN, MW, 30 min; ii. NaN_3, DMF, 90 °C.

Biological assessment

SPR measurement of DC-SIGN/BSA-man interaction in the presence of clusters 1, 2 and 3. Here we report the examination of the recognition behavior of ligands **1**, **2** and **3,** as well as the efficiency of the scaffold, for the inhibition of the extracellular domain (ECD) of DC-SIGN binding using a SPR competition assay. The sensor surface was grafted by bovine serum albumin protein bearing man1-3α[man1-6]man trisaccharide as a high mannose mimic of the HIV-1-gp120 glycoprotein (BSA-man).[42] Glycoconjugate affinities were determined by competition experiments following the reported procedure[54] by co-injection of 20 μM of DC-SIGN ECD and increasing concentrations of compounds **1**, **2** or **3** onto BSA-man. For sensorgrams of L-fucose as a positive monovalent control and for the three fucoclusters, see respectively tables 1, 2, 3, and 4 in SI. Figures 3A and 3B, respectively, show the inhibition curves and the corresponding IC_{50}. These demonstrated better apparent affinities with CRDs of DC-SIGN for fucocluster **1,** with an IC_{50} = 17 μM and multivalent power amplification represented by relative potency ($rp = IC_{50(\alpha\text{-L-fucose})}/IC_{50(\mathbf{1})}$) of about 120, with a high β avidity factor ($\beta = IC_{50(\mathbf{1})}/_{Valency\,=\,4}$) of about 30 compared to L-fucose (Table 1). The attachment of glycylglycyl-hydroxamic acid groups in *fuco* derivative **2** also keeps a favorable binding interaction with DC-SIGN. The IC_{50} is also strong (23.9

μM) and rp ($IC_{50(\alpha\text{-L-fucose})}/IC_{50(\text{Ligand } \mathbf{2})}$) and β avidity factors ($\beta = rp/_{\text{Valency} = 4}$) remain high (85 and 21 respectively), indicating a tight interaction compared to that of monovalent L-fucose. This finding evidenced a highly favorable topology impact compared to similar recent fucosylated dendrimers displaying higher level of multivalency.[55,56] For a better understanding of the phenomenon, we investigated water-soluble fucocluster **3** with the cone conformation that concentrates the four ligands at the down-rim of the calixarene ring. We observed a slight difference in IC_{50} values between clusters **1** (17 μM), **2** (23.9 μM) and **3** (26.5 μM), suggesting that both scaffold conformation impact similarly on the binding interaction. The high avidity observed, is due to the interaction of the sugar cap with DC-SIGN in solution via chelating and/or statistical binding rebinding mechanisms. Thiacalixarene or calixarene moieties contribute to the interaction with DC-SIGN by inducing high sugar densities via directional orientation of the sugar within a given set of distances between L-fucose units. Such results are reached with only four natural sugar units grafted onto the unusual thiacalixarene scaffold through an easy synthetic strategy that could be of interest in drug development. Importantly, inhibitory potencies towards DC-SIGN using fucoclusters **1** and **2** are around twenty times higher than other scaffolds with four natural ligands (D-Mann) or than highly *O*-fucosylated dendrimers.[57,58] We have demonstrated that DC-SIGN can be strongly inhibited, suggesting that a new generation of antiviral glycocluster-based thiacalixarene and calixarene scaffolds is possible. Results obtained with recombinant gB of the human cytomegalovirus (HCMV) envelope and against cis-infection of EBOV, the Zaïre species of Ebola virus (see below) supported this conclusion.

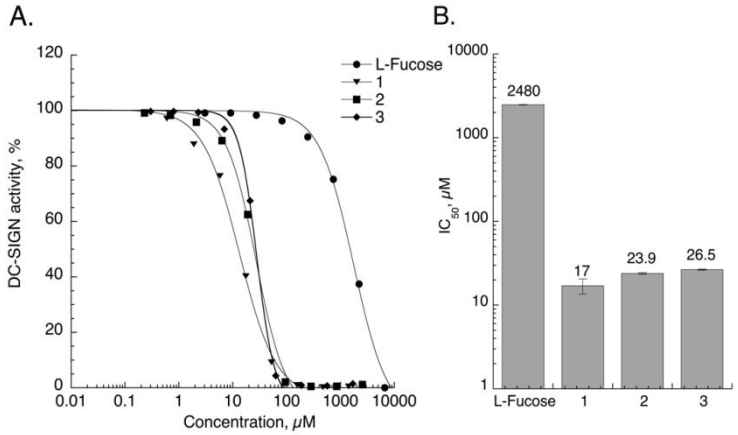

Figure 3. A. Inhibition curves of DC-SIGN binding to immobilized BSA-man (acting as an HIV-1-gp120 mimic) with L-Fucose (●) and clusters **1** (▼), **2** (■), or **3** (◆), using surface plasmon resonance (SPR). **B.** Histograms and the IC_{50} values of inhibition of DC-SIGN activity calculated for monovalent L-fucose and tetravalent fucoclusters **1**, **2** and **3**.

Table 1. IC_{50} of fucoclusters **1**, **2** and **3** for inhibition of DC-SIGN/BSA-man interaction. The results highlight the weak impact of topology, supporting the statistical rebinding or chelation interaction with the three ligands.

Compound	Valency	IC_{50} (μM)	Relative potency (rp)	β avidity factor
L-fucose	1	2048 ± 17.3	-	-
1	4	17 ± 0.4	120	30.12
2	4	23.9 ± 0.5	85.69	21.4
3	4	26.5 ± 0.5	93.58	19.32

$rp = IC_{50(L\text{-}fucose)}/IC_{50(Ligand\ \mathbf{1},\ \mathbf{2}\ or\ \mathbf{3})}$; β avidity factor = rp/n

Inhibition of HCMV recombinant gB /DC-SIGN-expressing U937 cell line by fucoclusters 1, **2 and 3**. Although HCMV is not as lethal as HIV-1(both viruses have spherical forms and highly mannosylated antigens) it causes lifelong infection in world population, serious congenital disease in new-borns and is responsible for dramatic chronic infections in immunocompromised individuals such as transplanted patients and those suffering from AIDS. As fin the case of HIV-1, there is no vaccine against HCMV, which in addition exhibits a growing resistance to existing treatments.[59] It is also known that HCMV requires iron for its cytomegaly development[60] and has the ability to penetrate a number of host cells and hijack their biochemical process for its replication.[61] One of the most important glycoprotein antigen in this respect is the highly mannosylated envelope glycoprotein B (gB)[62] used by HCMV to cross the external host cell membranes. Glycoprotein B is involved in two main ways: by interaction with DC-SIGN as the main mechanism for DCs infection[62,9] and by interaction with the host cell walls heparane sulfate to infect DCs and other cells.[61,63] Here, we focused on DC-SIGN which interacts with gB[64] in a similar manner as with the GP glycoprotein of Ebola virus or gp120 of HIV-1 during adhesion to host

cells, a step prior to infection. We demonstrated that gB/DC-SIGN binding is a fundamental interaction of the whole virus with DC-SIGN$^+$ cells, ie monocyte-derived DCs (MDDC) or U937 transfectants harboring DC-SIGN,[62] consequently its inhibition could be a serious mean to hinder HCMV trans-infection. The **1**, **2** and **3** fucoclusters seem to have the potential to inhibit HCMV trans-infection. The test used was based on the measurement of the interaction between human MDDC and one of their viral ligands, the recombinant form of gB. The inhibitors were tested with mannan as a positive control (Figure 4A). Our expectations were met since the HCMV recombinant gB/DC-SIGN interaction was inhibited at micromolar IC_{50} for fucocluster **1** (1 μM) and at submicromolar IC_{50} for cluster **3** (0.777 μM). We can consider these two activities as being similar. In contrast, a striking nanomolar IC_{50} (34 nM) was reached with cluster **2**-bearing hydroxamic acid groups (HAGs) (Figure 4A, Table 2). The three ligands show better inhibition than polymeric mannan, a known inhibitor of this interaction.[64] However, cluster **2** with the hydroxamic acid bearing linker deserves special mention, with inhibition that is 144-fold higher than mannan, and respectively 29- and 22-fold than fucocounterpart **1** and calix cone **3** (Table 2). Another striking observations is the efficient activity of **2** compared to the recently reported weak inhibitors harboring mannose units such tetravalent mannocluster based mannose as scaffold (higher than millimolar IC_{50})[65] or highly mannosylated polymer (89 mannose units, IC_{50} = 4.2 μM);[65] Cluster **2** is a 123-fold stronger inhibitor than the latter. Blocking HCMV gB/DC-SIGN binding in the nanomolar range is exceptional and shows that **1**, **3**, and to a large extent the fucocluster **2** prototype, have good spatial distributions that efficiently block the CRD sites of DC-SIGN. This reflects the intrinsic pre-organization of the thiacalixarene scaffold that acts synergistically through the contribution of the sugar units and the linkers carrying hydroxamic acid groups in **2**. The improved efficiency of glycocluster **2** might find its origin in another interaction, in addition to the one with DC-SIGN, with HCMV-gB itself thanks to the anionogenic property of the multiple hydroxamic acid assemblies. Indeed, It could mimick the HCMV-gB interaction with the negatively charge glycosaminoglycan sulfates of host cell walls..[61,63]

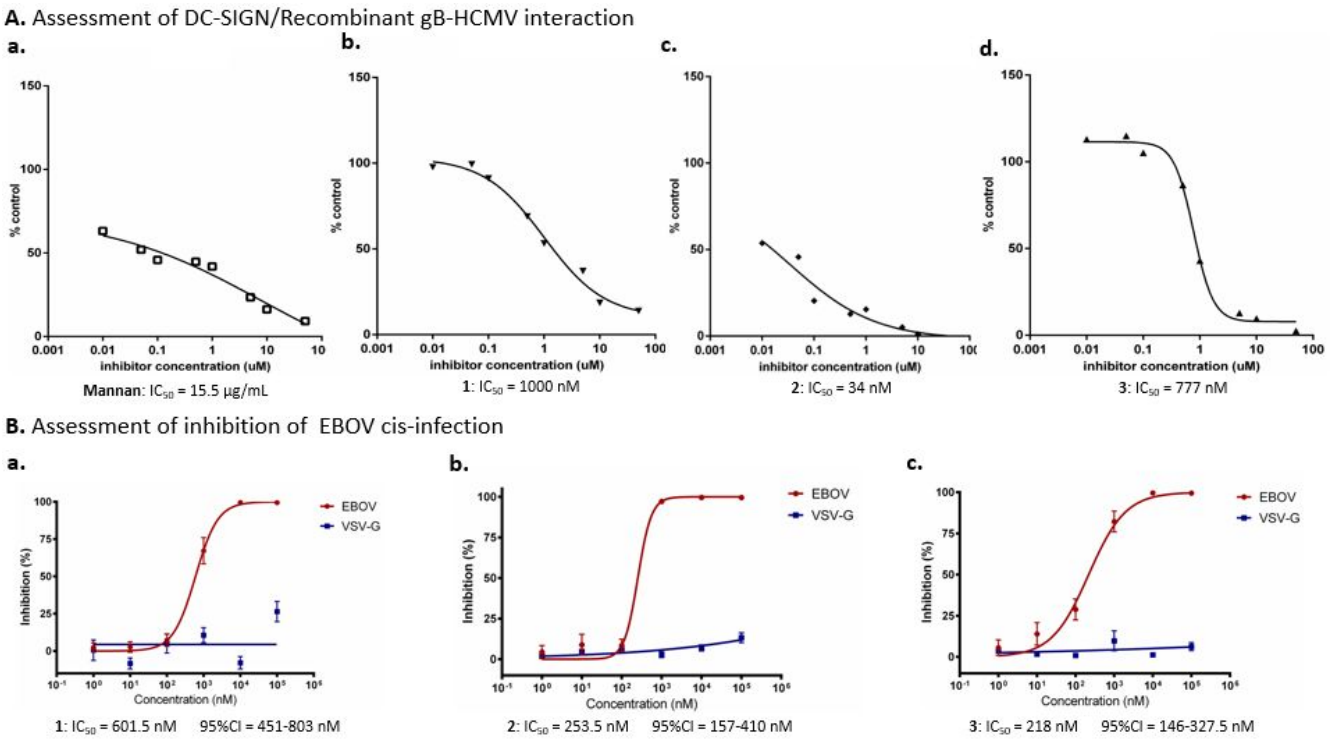

Figure 4. A. Inhibition curves of DC-SIGN/HCMV recombinant gB interaction obtained by flow cytometry with: **a.** Mannan, **b**. Fucocluster **1**, **c.** Fucocluster **2** and **d.** Fucocluster **3.** Duplicate experiment gave comparable results. **B.** Inhibition of EBOV pseudotyped virus cis-infection (●) using Jurkat cells expressing DC-SIGN. As reference VSV-GP (Vescicular Stomatitis virus envelope glycoprotein) (■) was used. Cells that do not express DC-SIGN were used as a negative control. EBOV inhibition by compounds: **a. 1**; **b. 2**; **c. 3** are shown. The three graphs **a**, **b** and **c** correspond to the mean of two independent experiments performed in triplicate with error bars corresponding to the standard errors of the mean.

Table 2. Summary of IC_{50} obtained for Inhibition of Interactions of DC-SIGN/clusters **1**, **2** and **3**, DC-SIGN/HCMV Recombinant gB and EBOV cis-Infection.

Compound	Valency	DC-SIGN/gB-HCMV interaction inhibition IC_{50}	Relative Inhibition/Mannan	Relative Inhibition of **2**/**1** and **2**/**3**	EBOV IC_{50} (nM)
Mannan		15.5 µg/mL	-	-	
1	4	1000 nM (3.155 µg/ml)	4.91	29/**1**	601.5
2	4	34 nM (0.107 µg/ml)	144	-	253.5
3	4	777 nM (2.400 µg/ml)	6.45	22/**3**	218

Inhibition of EBOV cis-infection by clusters 1, 2 and 3. The Ebola filovirus that is responsible for severe hemorrhagic fever[66,67] is dreaded worldwide due to its lethal action and the absence of efficient vaccines[68] and efficacious anti-infection strategies.[69,70] Of the five species identified by their region of origin, we were interested in the Zaire variant, now named Ebola virus (or EBOV) that causes up to 90% mortality and was responsible for the recent Ebola outbreak in West Africa.[71,72] Several therapeutic approaches have been attempted against Ebola virus infections such as the use of monoclonal antibodies[73] or small molecules that interfere with viral replication. However, despite some success of these molecules in preclinical models using non-human primates, there are currently no data to support their clinical efficacy.[74,75] The strategy of targeting an intracellular process is still threatened by the development of viral resistance, and the search for alternative strategies that would avoid such resistance remains limited. One possible unconventional approach is to prevent adhesion, communication and other infectious processes used by the virus, by acting exogenously. As DC-SIGN has been designed as a lead lectin with a function that is hijacked by EBOV for the recognition and subsequent infection of DC cells,[76] much work has been focused on the development of efficient multivalent inhibitors of this lectin to hinder binding of the virus to DCs. Several molecules have been assessed for their activity against EBOV,[36,58] and the best of these were highlighted in a recent perspective article.[36] However none was a glycocluster-based thiacalixarene or calixarene. Thus, we assessed glycoclusters **1**, **2** and **3** described in this paper against EBOV. Infection was performed on Jurkat cells (a T-lymphocyte cell line) expressing the DC-SIGN receptor. Since Ebola virus does not infect T-lymphocytes, its entry into Jurkat cells is absolutely dependent on DC-SIGN.[77] Jurkat DC-SIGN$^+$ cells were plated in 96-well plates and incubated at room temperature for 20 min with one of the three glycoclusters, and then challenged with 10000 TCID (Tissue culture infectious dose) of a recombinant virus pseudotyped with the Ebola virus envelope glycoprotein that expresses firefly luciferase.[78,79] After 48h, the cells were washed and lysed for a luciferase assay. The range of concentrations tested for the compounds was 1 nM–100 μM. As a control, an infection with VSV-G pseudo viruses (Vesicular stomatitis virus) was carried out under the same conditions. The infection with VSV-G is independent of the presence of the DC-SIGN receptor. The results of EBOV

inhibition by fucoclusters **1**, **2** and **3** are shown in figure 4B. Interestingly, all of compounds **1**, **2** and **3** exhibited strong inhibition of EBOV infection at an IC_{50} in the nanomolar scale (601.5, 253.5 and 218 nM respectively). It should be noted that fucocluster **3** is twice as effective as cluster **1** but acts quasi-equally to cluster **2**. Also, molecules **2** and **3** that only have four fucose units are more potent and stronger inhibitors of DC-SIGN-mediated EBOV infection than dendrimers with high densities of mannose units (e.g. the Boltorn dendrimer with 32 mannose units, IC_{50} = 337 nM).[76] This opens the way for further development of fucose-based antiviral thiacalixarene drugs against Ebola infection.

Conclusions

In conclusion, we have synthesized the first water-soluble thiacalix[4]arenes fucoclusters **1** and **2**, which are potent inhibitors of DC-SIGN. The evaluation in SPR competition experiments showed a unique affinity of soluble DC-SIGN for these clusters that is stronger than those reported for some *manno* or *fuco*-dendrimers with higher densities of mannose or fucose units. This supports the importance of the inherent directional presentation of sugars by the thiacalixarene scaffold. Nevertheless, the 1,3-alternate conformation seems not to be decisive since a similar result was obtained with the cone conformation of fucocluster **3**. This indifference with respect to conformation supports the possible occurrence of statistical association and/or chelation interaction with the possible existence of secondary interaction due to the functionalised linker. The latter interaction is probably responsible for the strong inhibition of both cis-infection by EBOV and of the interaction between recombinant HCMV gB and primary human cells like MDDC known to express DC-SIGN. The reached nanomolar avidity level in both cases may find its origin in a clustering binding mode, with the trans-membrane DC-SIGNs, in addition to the chelation and/or statistical rebinding observed in solution assays. Moreover, internalization of DC-SIGN upon binding, and its disappearance from the surface, may be also an enhancer of the inhibitory effect observed. Although these results need further investigation, it opens the way for further development of antiviral drugs based on these newly designed prototypes. The results of our research support also the conclusion

that anti-multi microbial treatment with a single drug is possible. We will investigated this in depth in our future program.

EXPERIMENTAL SECTION

1. Organic chemistry.

General methods. All chemical reagents were purchased from Sigma, Fisher (France) or TCI-Europe. ^{1}H and DeptQ NMR spectra were recorded on 600 MHz Bruker spectrometers in appropriate deuterated solvents; chemical shifts are reported on the δ scale. All ^{13}C NMR signals were assigned through C–H correlated HSQC spectra. TLC was performed on Silica Gel 60 F254, 230 mesh (E. Merck) with cyclohexane-EtOAc or EtOAc-MeOH, and spots were detected by vanillin–H_2SO_4 reagent. Preparative column chromatography was performed using 230–400 mesh Merck silica gel (purchased from Sigma). Flash chromatography was performed with Reveleris-Flash System apparatus with cartridge SiO_2-normal phase or C18-reverse phase. Low resolution electrospray mass spectra (ESI-MS) in the positive or negative ion mode were obtained on Waters ZQ 4000 quadrupole instrument equipped with an electrospray (Z-spray) ion source. High resolution electrospray experiments (ESI-HRMS) were performed on a Waters Q-TOF Ultima Global hybrid quadrupole time-of-flight instrument, equipped with an electro-spray (Z-spray) ion source.

Methyl *N*-(6-bromohexanoyl)-*N*-(prop-2-yn-1-yl)glycylglycinate (7). Formaldehyde (0.145 g; 4.84 mmol) and propargylamine (0.266 g; 4.84 mmol) in methanol (4 mL) were stirred at room temperature for 30 min. Then, methyl isocyanoacetate (0.4 g; 4.036 mmol) and 6-bromohexanoic acid (0.944 g; 4.84 mmol) were added. The resulted mixture was stirred at room temperature and followed by TLC until completion (36 h). After concentration, the residue was purified by flash chromatography (EtOAc/cyclohexane) affording the desired compound **7** as a yellow solid. Yield 0.973 g (67%); R_f = 0.25 (SiO_2, Cyclohexane/EtOAc : 3/2); ESI-MS: m/z = 385.0 $[M+Na]^+$. ^{1}H-NMR ($CDCl_3$, 600 MHz), δ (ppm): -6.94-6.78 (m, 1H, N<u>H</u>), 4.17-4.08 (m, 4H, C<u>H</u>$_2$C≡CH/NC<u>H</u>$_2$CO), 4.04-3.96 (m, 2H, NHC<u>H</u>$_2$CO), 3.70(s,

3H, OC$\underline{H}_3$), 3.49-3.25 (m, 2H, C$\underline{H}_2$Br), 2.51-2.22 (m, 3H, C$\underline{H}_2$/ $CH_2C{\equiv}C\underline{H}$), 1.84 (m, 2H, C$\underline{H}_2$), 1.66 (m, 2H, C$\underline{H}_2$), 1.46 (m, 2H, C$\underline{H}_2$). ^{13}C-NMR ($CDCl_3$, 150 MHz), δ (ppm): 173.5/173.2 ($\underline{C}$=O), 170.0/169.8 ($\underline{C}$=O), 169.0/168.5 ($\underline{C}$=O), 77.9 ($CH_2C{\equiv}\underline{C}H$), 73.3 ($CH_2\underline{C}{\equiv}CH$), 52.3 (O$\underline{C}H_3$), 49.4 (N$\underline{C}H_2CO$), 41.0 (NH$\underline{C}H_2CO$), 38.7 ($\underline{C}H_2$), 36.0 ($\underline{C}H_2$), 33.6 ($\underline{C}H_2$), 32.5 ($\underline{C}H_2$), 27.7 ($\underline{C}H_2$), 23.9 ($\underline{C}H_2$). HRMS(ESI/Q-TOF) m/z: $[M + Na]^+$ calcd for $C_{14}H_{21}BrN_2O_4Na$ 383.0582; found 383.0594.

Tetrabromo-tetramethylglycylglycinate pseudopeptide *p*-tBu-thiacalixarene 1,3-alternate derivative 8. To a stirred solution of compound **7** (0.48g; 1.32 mmol) and tetraazidopropyl-*p*-tBu-thiacalix[4]arene **6**[39] (0.318g; 0.301 mmol) in THF/tBuOH (7.5mL/15mL) was added a freshly prepared solution of Cu(I) (from $CuSO_4.5H_2O$ (0.15 g) and sodium ascorbate (0.239 g) in H_2O (15 mL)). The mixture was stirred for 3h at 60 °C. After solvent evaporation, the crude product was extracted with CH_2Cl_2 and washed with brine. The organic layer was dried on $MgSO_4$ and concentrated. Compound **8** was obtained after purification by column chromatography on silica gel (3/3/2: acetone/EtOAc/Cyclohexane, 1% $N(Et)_3$) as a white solid. Yield 0.396 g (58%); R_f = 0.43 (SiO_2, acetone/EtOAc/Cyclohexane : 2/2/1 + 1% $N(Et)_3$); ESI-MS: m/z = 1272.3 $[M+2Na]^{2+}$. ^{1}H-NMR ($CDCl_3$, 600 MHz), δ(ppm): 7.95-7.55 (m, 8H , N$\underline{H}$/C$\underline{H}_{triazole}$), 7.27-7.21 (m, 8H, C$\underline{H}$Ar), 4.73-4.56 (m, 8H, C$\underline{H}_2$), 4.28-3,90 (m, 40H, C$\underline{H}_2$), 3.70 (s, 12H, OC$\underline{H}_3$), 3.36 (t, 8H, C$\underline{H}_2$Br, J = 6.7 Hz), 2.60-2.25 (m, 8H,C$\underline{H}_2$), 1.87-1.79 (m, 8H, C$\underline{H}_2$), 1.74-1.54 (m, 16H, C$\underline{H}_2$), 1.54-1.39 (m, 8H,C$\underline{H}_2$), 1.01 (s, 36H, C$\underline{H}_3$). ^{13}C-NMR ($CDCl_3$, 150 MHz), δ(ppm): 174.0-168.8 ($\underline{C}$=O), 156.3 (Ar$\underline{C}$OCH$_2$), 146.3 (Ar$\underline{C}$(C(CH$_3$)$_3$)), 143.4 ($C_{triazole}$), 128.1 **(**Ar$\underline{C}$S$\underline{C}$Ar**)**, 127.3 ($\underline{C}$HAr), 122.9 ($\underline{C}H_{triazole}$), 66.0 ($\underline{C}H_2$OAr), 52.3 (O$\underline{C}H_3$), 51.6 ($\underline{C}H_2$), 50.1 ($\underline{C}H_2$),47.8 ($\underline{C}H_2$), 44.6 ($\underline{C}H_2$), 42.5 ($\underline{C}H_2$), 41.0 ($\underline{C}H_2$), 34.1 ($\underline{C}(CH_3)_3$), 32.5 ($\underline{C}H_2$), 31.0 ($\underline{C}H_3$), 30.0 ($\underline{C}H_2$), 27.7 ($\underline{C}H_2$), 24.0 ($\underline{C}H_2$). HRMS(ESI/Q-TOF) m/z: $[M+2Na]^{2+}$ calcd for $C_{108}H_{152}Br_4N_{20}Na_2O_{20}S_4$ 1269.3451 found: 1269.3447.

Tetrazido-tetramethylglycylglycinate-pseudopeptide *p*-tBu-thiacalixarene 1,3-alternate derivative 9. To a stirred solution of compound **8** (0.375g; 0.15 mmol) in DMF (12 mL) was added NaN_3 (0.117g; 1.79 mmol). After 12 h at 90 °C and evaporation, the crude product was extracted with CH_2Cl_2 and washed

with brine. The organic layer was dried on $MgSO_4$ and concentrated. Compound **9** was obtained after purification by column chromatography on silica gel (3/3/2: acetone/EtOAc/Cyclohexane, 1% $N(Et)_3$) as a yellow solid. Yield 0.324 g (92 %); R_f = 0.43 (SiO_2, acetone/EtOAc/Cyclohexane : 2/2/1 + 1% $N(Et)_3$); ESI-MS: m/z = 1196.0 $[M+Na]^{2+}$. ^{1}H-NMR ($CDCl_3$, 600 MHz), δ (ppm): 8.00-7.56 (m, 8H , N<u>H</u>/C<u>H</u>$_{triazole}$), 7.26-7.20 (s, 8H, C<u>H</u>Ar), 4.71-4.49 (m, 8H, C<u>H</u>$_2$), 4.28-3.89 (m, 40H, C<u>H</u>$_2$), 3.69 (s, 12H, OC<u>H</u>$_3$), 3.23(m, 8H, C<u>H</u>$_2$N$_3$), 2.64-2.22 (m, 8H,C<u>H</u>$_2$), 1.87-1.79 (m, 8H, C<u>H</u>$_2$), 1.74-1.56 (m, 16H, CH_2), 1.47-1.33 (m, 8H,C<u>H</u>$_2$), 0.98 (s, 36H, C<u>H</u>$_3$). ^{13}C-NMR ($CDCl_3$, 150 MHz), δ (ppm): 174.1-173.4 (<u>C</u>=O), 170.4- 168.7 (<u>C</u>=O), 156.3 (Ar<u>C</u>OCH$_2$), 146.3 (Ar<u>C</u>(C(CH$_3$)$_3$)), 143.6 (<u>C</u>$_{triazole}$), 128.1 **(**Ar<u>C</u>S<u>C</u>Ar**)**, 127.3 (<u>C</u>HAr), 123.07 (<u>C</u>H$_{triazole}$), 66.1 (<u>C</u>H$_2$OAr), 52.2 (O<u>C</u>H$_3$), 51.4 (<u>C</u>H$_2$N$_3$), 50.1 (<u>C</u>H$_2$),47.5 (<u>C</u>H$_2$), 44.5 (<u>C</u>H$_2$), 42.5 (<u>C</u>H$_2$), 41.0 (<u>C</u>H$_2$), 34.1 (<u>C</u>(CH$_3$)$_3$), 32.7 (<u>C</u>H$_2$), 31.2 (<u>C</u>H$_3$), 29.8 (<u>C</u>H$_2$), 28.6 (<u>C</u>H$_2$), 26.3 (<u>C</u>H$_2$). HRMS(ESI/Q-TOF) m/z: $[M+2Na]^{2+}$ calcd for $C_{108}H_{152}N_{32}O_{20}S_4Na_2$ 1195.5264, found: 1195.5250.

Peracetylated tetramethylglycylglycinate-pseudopeptide *p*-tBu-thiacalixarene 1,3-alternate derivative 11. To a stirred solution of thiacalix **9** (0.2 g; 0.085 mmol) and acetylated α-L-fucose **10** (0.123 g; 0.374 mmol) in THF/tBuOH (8mL/16mL) was added a freshly prepared solution of Cu(I) (from $CuSO_4.5H_2O$ (0.042g) and sodium ascorbate (0.067g) in H_2O (16 mL)). The mixture was stirred for 3h at 60 °C. After solvent evaporation, the crude product was extracted with CH_2Cl_2 and washed with brine. The organic layer was dried on $MgSO_4$ and concentrated. Compound **11** was obtained after purification by column chromatography on silica gel (3/3/1.5: acetone/EtOAc/cyclohexane, 1% $N(Et)_3$) as a white solid. Yield 0.193 g (62%); R_f = 0.2 (SiO_2, acetone/EtOAc/Cyclohexane : 3/3/1.5 + 1% $N(Et)_3$); ESI-MS: m/z = 1853.1 $[M+2Na]^{2+}$. ^{13}C-NMR ($CDCl_3$, 150 MHz), δ (ppm): 174.9-174.4 (<u>C</u>=O), 171.9-169.7 (<u>C</u>=O), 143.7 (<u>C</u>$_{triazole}$), 123.6 (CH$_{triazole}$), 122.8 (<u>C</u>HAr), 95.6 (C-1), 71.1, 68.0, 64.7(C-2, C-3, C-4, C-5), 61.2 (<u>C</u>H$_2$OAr/<u>C</u>H$_2$Otriazole) 51.8 (O<u>C</u>H$_3$), 50.1 (<u>C</u>H$_2$N$_3$), 41.0 (<u>C</u>H$_2$), 32.7 (<u>C</u>H$_2$), 31.2 (<u>C</u>H$_3$), 29.3 (<u>C</u>H$_2$), 25.9 (<u>C</u>H$_2$), 24.3 (<u>C</u>H$_2$), 20.7 (<u>C</u>H$_2$),15.8 (C-6). HRMS(ESI/Q-TOF) m/z: $[M+2Na]^{2+}$ calcd for $C_{168}H_{232}N_{32}Na_2O_{52}S_4$ 1851.7586, found 1851.7592

Tetramethylglycylglycinate-pseudopeptide *p*-tBu-thiacalixarene fucocluster 1,3-alternate 1. To a stirred solution of thiacalix **9** (0.320 g; 0.136 mmol) and compound **12** (0.121 g; 0.59 mmol) in THF/tBuOH/MeOH (5mL/5mL/5mL) was added a freshly prepared solution of Cu(I) (from $CuSO_4.5H_2O$ (0.073 g) and sodium ascorbate (0.116 g) in H_2O (5 mL)). The mixture was stirred for 3h at 60 °C. The resulting crude was purified by reverse-phase chromatography with eluent gradient of H_2O/CH_3CN to afford **1** as a yellow solid. Yield 0.229 g (53%); ESI-MS: m/z = 1600.7 $[M+2Na]^{2+}$. ^{1}H-NMR (MeOD, 600 MHz), δ (ppm): 7.96-7.74 (m, 8H , NH/$CH_{triazole}$), 7.27 (s, 8H, CHAr),4.79-7.70 (m, 4H, H-1), 4.69-4.50 (m, 16H, OCH_2triazole /CH_2), 4.28 (m, 8H, CH_2), 4.25-3.98 (m, 16H, CH_2/CH_{Fuc}), 3.97-3.74 (m, 12H, CH_2/H_{Fuc}), 3.66-3.55 (m, 24H, CH_2), 3.25 (s, 12H, OCH_3), 3.21 (s, 4H,H_{Fuc}), 2.58-2.12 (m, 8H,CH_2), 1.98-1.71 (m, 8H,CH_2), 1.67-1.46 (m, 16H, CH_2), 1.30-1.16 (m, 8H, CH_2), 1.07 (d, 12H, H-6, J = 5.9 Hz), 0.99 (s, 36H, CH_3). ^{13}C-NMR (MeOD, 150 MHz), δ (ppm): 174.5-174.3 (C=O), 170.4-169.8 (C=O), 156.4 ($ArCOCH_2$), 146.5 ($ArC(C(CH_3)_3)$), 144.2 ($C_{triazole}$), 128.1 **(**ArCSCAr**)**, 127.2 (CHAr), 123.70 ($CH_{triazole}$), 98.7 (C-1), 72.2, 70.2, 68.5, 66.5 (C-2, C-3, C-4, C-5), 65.8 (CH_2OAr), 60.3 (OCH_2triazole), 51.4 (OCH_3), 50.2 (CH_2), 49.2 (CH_2), 43.7 (CH_2), 41.7 (CH_2), 40.5(CH_2), 33.8 ($C(CH_3)_3$), 32.1 (CH_2), 30.3 (CH_3), 29.6 (CH_2), 25.6 (CH_2), 24.0 (CH_2),15.3 (C-6). HRMS(ESI/Q-TOF) m/z: $[M+2Na]^{2+}$ calcd for $C_{144}H_{208}N_{32}O_{40}S_4Na_2$ 1599.6952, found: 1599.6948.

Tetrahydroxamic acid glycylglycinate-pseudopeptide *p*-tBu-thiacalixarene fucocluster 1,3-alternate 2. Compound **1** (0.100g; 0.031 mmol), NH_2OH (50%) (0.012 g; 0.38 mmol) and KCN (0.003 g; 0.05 mmol) were dissolved in THF/MeOH (0.3 mL/0.3 mL) solvent mixture and stirred 7h at room temperature. The resulting crude was purified by reverse-phase chromatography with eluent gradient of H_2O/CH_3CN to afford **2** as a yellow solid. Yield 0.054 g (54%); ESI-MS: m/z = 1602.8 $[M+2Na]^{2+}$. ^{1}H-NMR (MeOD, 600 MHz), δ (ppm): 8.22-7.9 (m, 8H , NH/$CH_{triazole}$), 6.86 (s, 8H, CHAr), 4.93-4.52 (m, 28H, H-1/OCH_2triazole/CH_2), 4.40-4.27 (m, 24H, CH_2), 4.03-3.85 (m, 48H, CH_{Fuc}/CH_2), 2.71-2.40 (m, 16H, CH_2), 2.35 (m, 4H, CH_2), 1.91(m, 8H, CH_2), 1.64 (m, 8H, CH_2), 1.35 (m, 8H,CH_2), 1.19 (d, 12H, H-6, J = 6.1 Hz), 1.10 (s, 36H, CH_3). ^{13}C-NMR (MeOD, 150 MHz), δ (ppm): 175.9 (C=O), 171.7-171.0 (C=O), 154.3 ($ArCOCH_2$), 146.1 ($ArC(C(CH_3)_3)$), 134.8 **(**ArCSCAr**)**, 126.4 (CHAr), 125.2 ($CH_{triazole}$),

100.1 (C-1), 73.3 , 73.0($\underline{C}H_2OAr$), 71.5, 69.9, 67.8(C-2, C-3, C-4, C-5), 61.7 ($O\underline{C}H_2$triazole), 51.6 ($\underline{C}H_2$), 51.2 ($\underline{C}H_2$), 45.2 ($\underline{C}H_2$), 41.8 ($\underline{C}H_2$), 41.8 ($\underline{C}H_2$), 34.8 ($\underline{C}(CH_3)_3$), 33.6 ($\underline{C}H_2$), 32.0 ($\underline{C}H_2$), 30.97 ($\underline{C}H_3$), 27.0 ($\underline{C}H_2$), 25.3 ($\underline{C}H_2$), 16.7 (C-6). HRMS(ESI/Q-TOF) m/z: $[M+2Na]^{2+}$ calcd for $C_{140}H_{204}N_{36}Na_2O_{40}S_4$ 1601.6857, found 1601.6855.

Tetrabromo-tetramethylglycylglycinate-pseudopeptide *p*-tBu-calix[4]arene derivative 14. To a stirred solution of compound **7** (0.291g; 0.807 mmol) and tetraazidocalix **13** (0.180 g; 0.183 mmol) in THF/tBuOH (7.5mL/15mL) was added a freshly prepared solution of Cu(I) (from $CuSO_4.5H_2O$ (0.091 g) and sodium ascorbate (0.145 g) in H_2O (15 mL)). The mixture was stirred for 3h at 60 °C. After solvent evaporation, the crude product was extracted with CH_2Cl_2 and washed with brine. The organic layer was dried on $MgSO_4$ and concentrated. Compound **14** was obtained after purification by column chromatography on silica gel (2/2/1: acetone/EtOAc/Cyclohexane, 1% $N(Et)_3$) as a white solid. Yield 0.253 g (57%); R_f = 0.12 (SiO_2, acetone/EtOAc/Cyclohexane, 2/2/1 + 1% $N(Et)_3$); ESI-MS: m/z = 1235.9 $[M+2Na]^{2+}$. ^{1}H-NMR ($CDCl_3$, 300 MHz), δ (ppm): 8.1-7.6 (m, 8H, N$\underline{H}$/ C$\underline{H}_{triazole}$), 6.77 (m, 8H, C$\underline{H}$Ar), 4.52-4.34 (m, 8H, C$\underline{H}_2$), 4.30-4.11 (m, 12H, C$\underline{H}_2$/ArC$\underline{H}_2$Ar), 4.01 (m, 8H, C$\underline{H}_2$), 3.91 (m, 8H, C$\underline{H}_2$), 3.73-3.63 (m, 12H, OC$\underline{H}_3$), 3.38 (m, 8H, C$\underline{H}_2$), 3.15 (dd, 4H, ArC$\underline{H}_2$Ar , *J* = 12,3 Hz), 2.61-2.44 (m, 12H, C$\underline{H}_2$), 2.32 (m, 4H, C$\underline{H}_2$), 1.83 (m, 8H, C$\underline{H}_2$), 1.58 (m, 8H, C$\underline{H}_2$), 1.41 (m, 8H, C$\underline{H}_2$), 1.05 (m, 36H, C$\underline{H}_3$). ^{13}C-NMR ($CDCl_3$, 75 MHz), δ (ppm) : 174.1-173.7 ($\underline{C}$=O), 170.4-169.1 ($\underline{C}$=O), 152.8 (Ar$\underline{C}OCH_2$), 145.3 (Ar$\underline{C}(C(CH_3)_3)$), 143.7 ($C_{triazole}$), 133.2 **(**Ar$\underline{C}CH_2\underline{C}$Ar**)**, 125.4 ($\underline{C}$HAr), 123.52 ($\underline{C}H_{triazole}$), 71.8 ($O\underline{C}H_2$), 51.9($O\underline{C}H_3$), 47.8 ($\underline{C}H_2$), 44.5 ($\underline{C}H_2$), 41.1 ($\underline{C}H_2$), 33.8 ($\underline{C}H_2$), 32.8 ($\underline{C}H_2$), 32.6 ($\underline{C}H_2$Br), 31.4($\underline{C}H_3$), 31.1 ($\underline{C}H_2$), 27.8 ($\underline{C}H_2$), 24.1 ($\underline{C}H_2$). HRMS(ESI/Q-TOF) m/z: $[M+2Na]^{2+}$ calcd for $C_{112}H_{160}Br_4N_{20}Na_2O_{20}$ 1233.4324, found 1233.4350.

Tetraazido-tetramethylglycylglycinate-pseudopeptide *p*-tBu-calix[4]arene derivative 15. To a stirred solution of compound **14** (0.240 g; 0.099 mmol) in DMF (12 mL) was added NaN_3 (0.077g; 1.186 mmol). After 12 h at 90 °C and evaporation, the crude product was extracted with CH_2Cl_2 and washed with brine. The organic layer was dried on $MgSO_4$ and concentrated. Compound **15** was obtained after purification by column chromatography on silica gel (2/2/1 : acetone/EtOAc/Cyclohexane, 1% $N(Et)_3$) as a yellow

solid. Yield 0.213 g (95 %); R_f = 0.14 (SiO_2, acetone/ EtOAc/ Cyclohexane : 2/2/1 + 1% $N(Et)_3$). ESI-MS: m/z = 1160.1 $[M+Na]^{2+}$. ^{1}H-NMR ($CDCl_3$, 300 MHz), δ (ppm): 8.30-7.3 (m, 8H, C$\underline{H}_{triazole}$/ NH), 6.74 (m, 8H, C$\underline{H}$ Ar), 4.54-4.31 (m, 8H, C$\underline{H}_2$), 4.28-4.11 (m, 12H, ArC$\underline{H}_2$Ar/C$\underline{H}_2$), 4.08-3.94 (m, 8H, C$\underline{H}_2$), 3.96-3.78 (m, 8H, C$\underline{H}_2$O), 3.63(m, 12H,OC$\underline{H}_3$), 3.28-3.02 (m, 12H , CH_2/ArC$\underline{H}_2$Ar), 2.65-2.22 (m, 8H, C$\underline{H}_2$),1.72-1.44(m, 8H, C$\underline{H}_2$), 1.49-1.25 (m, 8H, C$\underline{H}_2$), 1.03 (m, 36H, C$\underline{H}_3$). ^{13}C-NMR ($CDCl_3$, 75 MHz), δ (ppm) : 174.0/173.8 (C$\underline{=}$O), 170.2/170.0 (C$\underline{=}$O), 169.7/169.2 (C$\underline{=}$O), 158.0 (ArCOCH$_2$), 145.2 (ArC(C(CH$_3$)$_3$)), 143.2 (C$_{triazole}$), 133.1 **(**ArCCH$_2$CAr**)**, 125.3 (CHAr), 123.21 (CH$_{triazole}$), 71.8 (OCH$_2$), 52.2 (OCH$_3$), 51.2 (CH$_2$N$_3$), 47.7 (CH$_2$), 46.0 (CH$_2$), 41.0 (CH$_2$), 33.8 (C(CH$_3$)$_3$), 32.7 (CH$_2$), 31.3 (CH$_3$), 31.0 (CH$_2$), 29.6 (CH$_2$), 28.4 (CH$_2$), 26.3 (CH$_2$), 24.4 (CH$_2$). HRMS(ESI/Q-TOF) m/z: $[M+2Na]^{2+}$ calcd for $C_{112}H_{160}Br_4N_{32}O_{20}Na_2$ 1159.6135, found: 1159.6150.

Tetramethylglycylglycinate-pseudopeptide *p*-tBu-calix[4]arene fucocluster 3. To a stirred solution of calix **15** (0.32 g; 0.140 mmol) and compound **12** (0.125 g; 0.618 mmol) in THF/tBuOH/MeOH (5mL/5Ml/5mL) was added a freshly prepared solution of Cu(I) (from $CuSO_4.5H_2O$ (0.070g) and sodium ascorbate (0.111g) in H_2O (5 mL)). The mixture was stirred for 3h at 60 °C. The resulting crude was purified by reverse-phase chromatography with eluent gradient of H_2O/CH_3CN to afford **3** as a yellow solid. Yield 0.211 g (49%); ESI-MS: m/z = 1564.8 $[M+2Na]^{2+}$. ^{1}H-NMR (MeOD, 600 MHz), δ (ppm): 8.19-8.00 (m, 8H, C$\underline{H}_{triazole}$/N$\underline{H}$), 6.86 (m, 8H, C$\underline{H}$ Ar), 4.81-4.55 (m, 20H, H-1/OC$\underline{H}_2$triazole /CH$_2$), 4.45-4.28 (m, 12H, C$\underline{H}_2$/ArC$\underline{H}_2$Ar), 4.18 (m, 8H, C$\underline{H}_2$), 3.99-3.94 (m, 12H, C$\underline{H}_2$/H$_{Fuc}$), 3.90 (m, 8H, C$\underline{H}_2$OAr), 3.76 (s, 2H, H$_{Fuc}$), 3.72-3.65 (m, 16H, OC$\underline{H}_3$/H$_{Fuc}$), 3.15 (d, 4H, ArC$\underline{H}_2$Ar, J =11.9 Hz), 2.54 (m, 16H, C$\underline{H}_2$), 1.89 (m, 8H, C$\underline{H}_2$), 1.64 (m, 8H, C$\underline{H}_2$), 1.34 (m, 8H, C$\underline{H}_2$), 1.19 (d, 12H, H-6, J = 6.1 Hz), 1.10 (m, 42H, C$\underline{H}_3$/C$\underline{H}_2$). ^{13}C-NMR (MeOD, 150 MHz), δ (ppm): 175.6 (C$\underline{=}$O), 171.6-171.0 (C$\underline{=}$O), 154.0 (ArCOCH$_2$), 145.9 (ArC(C(CH$_3$)$_3$)), 134.6 **(**ArCCH$_2$CAr**)**, 126.2 (CHAr), 124.9 (C$\underline{H}_{triazole}$), 99.9 (C-1), 73.4, 72.8 (C$\underline{H}_2$OAr), 71.3, 69.7, 67.6 (C-2, C-3, C-4, C-5), 61.5 (OC$\underline{H}_2$triazole), 52.5 (C$\underline{H}_2$), 51.4 (C$\underline{H}_2$), 50.9 (C$\underline{H}_2$), 41.6 (C$\underline{H}_2$), 34.5 (C(CH$_3$)$_3$), 33.4 (C$\underline{H}_2$), 33.3 (C$\underline{H}_2$), 31.8 (C$\underline{H}_2$), 31.7 (C$\underline{H}_3$), 30.7 (C$\underline{H}_2$), 26.7 (C$\underline{H}_2$), 25.1 (C$\underline{H}_2$), 16.4 (C-6). HRMS(ESI/Q-TOF) m/z: $[M+2Na]^{2+}$ calcd for $C_{148}H_{216}N_{32}Na_2O_{40}$ 1563.7824, found 1563.7870.

2. Biological assessments.

SPR experiments measurement of DC-SIGN/ligands 1, 2 and 3 interaction. DC-SIGN ECD production and purification. DC-SIGN extracellular domain (DC-SIGN ECD) construct was produced and purified as described previously.[54] Surface Plasmon Resonance analysis (SPR). competition assay. SPR experiments were performed on a Biacore 3000 using a CM4 chip, functionalized at 5 µL/min. BSA or BSA-Man were immobilized on flow cells using amine-coupling method. Fc1 was prepared as reference surface. Flow cell (Fc) 1, 2, 3 and 4 were acti- vated with 50 µL of a 0.2 M EDC/0.05 M NHS mixture. Fc1 was functionalized with bovine serum albumine (BSA), while Fc2, Fc3 and Fc4 were functionalized with mannosylated bovine serum albumine (BSA-(Manα1-3[Manα1-6]Man) from Dextra laboratories. Remaining activated groups were blocked with 30 µL of 1 M ethanolamine. After blocking, the four Fc were treated with 5 µL of 10 mM HCl to remove unspecific bound protein and 5 µL of 50 mM Na_2EDTA to expose surface to regeneration protocol. The final immobilization levels for the Fc1, 2, 3 and 4 are respectively 1541 RU, 1664 RU, 1376 RU and 1847 RU. For inhibition studies, 20 µM of DC-SIGN ECD mixed with increasing concentrations of inhibiting compounds were prepared in a running buffer composed of 25 mM Tris pH 8, 150 mM NaCl, 4 mM $CaCl_2$, 0.005% P20 surfactant, and 13 µL of each sample was injected onto the surfaces at a 5 µL/min flow rate. The resulting sensorgrams were reference surface corrected. The DC-SIGN binding responses were extracted from sensorgrams, converted to percent residual activity values (y) with respect to lectin alone binding, and plotted against corresponding compound concentration. The 4-parameter logistic model (See SI equation 1) was fitted to the plots, and the IC_{50} values were calculated using the values of fitted parameters (R_{hi}, R_{lo}, A_1 and A_2) (See SI equation 2).

Inhibition of DC-SIGN/HCMV recombinant gB glycoprotein interaction. U937 parental cells (ATCC® CRL-1593.2™, LGC Standards, UK) or stably expressing the full length DC-SIGN lectin were propagated in RPMI 1640, 2mM glutamine, 10% FCS (HyClone/GE Healthcare, Wauwatosa, WI). Cells were resuspended in the binding buffer, TBS, 1 mM $CaCl_2$, 2mM $MgCl_2$, 0.1% bovine serum albumin (BSA) and then seeded in 96-well plates at 1.10^5 cells per well and Alexa 488®-conjugated recombinant HCMV gB (2 µg/ml) was then added to cells for 20 min at 4°C. Cells were washed thoroughly with cold binding buffer before being analyzed on a LSR II flow cytometer (BD Biosciences, Franklin Lakes, NJ) and the Flow Jo software (Tree Star, Ashland, OR).

Inhibition of EBOV cell line trans-infection. Recombinant viruses were produced in 293T cells by transfection with Lipofectamine 2000 (Life Technologies) following the manufacturer´s protocol. The viral construction was pseudotyped with Ebola virus (EBOV) envelope glycoprotein (GP) or Vesicular Stomatitis virus envelope GP (VSV-G) and expressed luciferase as a reporter of the infection.[78,79] One day (18-24 h) before transfection, 5 x 10^6 293T were seeded onto 10 cm plates. Cells were cultured in DMEM medium supplemented with 10% heat-inactivated FBS, 25 mg Gentamycin, 2 mM L-glutamine. Supernatants containing GP-pseudotyped viruses were harvested 48h later, centrifuged to remove cell debris and stored in aliquots at -80º C. Infectious titers were estimated as tissue culture infectious dose per mL by limiting dilution of the lentivirus-containing supernatants on HeLa cells. Luciferase activity was determined by luciferase assay (Luciferase Assay System, Promega, Madison, WI) in a GloMax®-Multi+ Detection System (Promega, Madison, WI, USA).

3. MMFF computational calculation. *Spartan '14* software was used to generate 6561 conformers of the **2** thiacalix[4]arene repeat unit (*O*-alkylated 4-(tert-butyl)-2-mercaptophenol) in the gas phase. The relative steric energy of each conformer was determined by molecular mechanics using the Merck Molecular Force Field (MMFF) and the lowest 100 conformers were retained. The lowest energy conformer was replicated four times and linked to reform the thiacalix[4]arene. MMFF was used to optimize the geometry of the macrocycle. The resulting structure is as shown. It is notable that the most stable substituent conformer is very compact with dimensions down the axis of the thiacalixarene cavity of about 17 Å with dimensions perpendicular to the thiacalix[4]arene axis of 31 Å x 31

Å. None of the 100 lowest energy structures retained during analysis represented an extended conformer of the single repeat unit so one was constructed through forced bond rotation. Following geometry optimisation (MMFF) the structure was replicated and the extended form of the thiacalix[4]arene generated. Final geometry optimisation by MMFF gave the extended structure shown. Here the length of the thiacalixarene down the thiacalix[4]arene axis was approximately 55 Å (See SI, Figure S31**)** with perpendicular dimensions of 12 Å x 12 Å at the macrocycle's annulus and 21 Å x 4 Å where the hydroxamic acid side arms emerge from the lower rim substituents.

ASSOCIATED CONTENT

Supporting Information. NMR and LC-MS data; Figure obtained from SPR; Figure obtained from MMFF; This material is available free of charge via the Internet at http://pubs.acs.org."

AUTHOR INFORMATION

Corresponding Author

* E-mail: mohammed.benazza@u-picardie.fr

* E.mail: E-mail: franck.fieschi@ibs.fr

Author Contributions

The manuscript was written through contributions of all authors. All authors have given approval to the final version of the manuscript. [£]These authors contributed equally.

Funding Sources

The authors declare no competing financial interest.

ACKNOWLEDGMENT

Suport from the "Conseil Régional de Picardie" and the LG2A-UMR7378-CNRS research group is gratefully acknowledged. M. Taouai and K. Chakroun were financially supported by the Tunisian government. V. Porkolab was supported by la Région Rhône-Alpes. This work used the platforms of the Grenoble Instruction center (ISBG; UMS 3518 CNRS-CEA-UGA-EMBL), notably SPR and MP3 platforms, with support from FRISBI (ANR-10-INSB-05-02) and GRAL (ANR-10-LABX- 49-01) within

the Grenoble Partnership for Structural Biology (PSB). F. Fieschi thanks for the support of the French Agence Nationale de la Recherche (ANR) PIA for Glyco@Alps (ANR- 15-IDEX-02). R. Delgado's research was funded by the Fondo de Investigación Sanitaria (FIS-ISCIII) through grants PI140078 and DTS1500171). We thank the "Développement et Transfert à la Clinique platform (http://www.cicnantes.fr/fr/component/glossary/Glossaire-1/C/CIC-35/, CIC Biothérapies CBT 0503, CHU Nantes, France)" for providing elutriated monocytes, clinical grade cytokines, and human serum albumin. The ARMINA Consortium (no. 2012 09680) supported Coraline Chéneau's salary.

ABBREVIATIONS

DC-SIGN, dendritic cell-specific intercellular adhesion molecule-3-grabbing non-integrin; SPR , surface plasmon resonance; BSA, bovine serum albumin; HCMV, human cytomegalovirus; gB, glycoprotein B; EBOV, ebola virus; VSV, vesicular stomatitis virus; Ugi-4CR , Ugi four component reaction; HAGs, hydroxamic acid groups; MBL, mannose binding lectins. TCID, tissue culture infectious dose; MMFF, molecular Mechanic Force Field; MDDC, monocyte-derived dendritic cells; DC, dendritic cell; ECD, extra-cellular domain; CRD, carbohydrate recognition domain; ICAM3, Intercellular adhesion molecule 3. HIV-1, human immunodeficiency virus 1; SARS, severe acute respiratory syndrome. DMEM, dulbecco's modified eagle's medium; DIEA, diisopropylethylamine; DMF, dimethylformamide.

REFERENCES

(1) Lozano, R., Naghavi, M., Foreman, K., Lim, S., Shibuya, K., Aboyans, V., Abraham, J., Adair, T., Aggarwal, R., and Ahn, S. Y. (2012) Global and regional mortality from 235 causes of death for 20 age groups in 1990 and 2010: a systematic analysis for the Global Burden of Disease Study 2010. *The lancet 380*, 2095-2128.

(2) De Clercq, E., and Herdewijn, P. (2010) Strategies in the design of antiviral drugs. *Pharm. Sci. Encyclop.: Drug Discov. Develop. Manufact.*, 1-56.

(3) De Clercq, E., and Li, G. (2016) Approved antiviral drugs over the past 50 years. *Clin. Microbiol. Rev. 29*, 695-747.

(4) Shankar, E. M., Vignesh, R., EllegAard, R., Barathan, M., Chong, Y. K., Bador, M. K., Rukumani, D. V., Sabet, N. S., Kamarulzaman, A., and Velu, V. (2014) HIV–Mycobacterium tuberculosis co-infection: a 'danger-couple model'of disease pathogenesis. *Pathog. Dis. 70*, 110-118.

(5) Kovacs, A., Schluchter, M., Easley, K., Demmler, G., Shearer, W., Russa, P. L., Pitt, J., Cooper, E., Goldfarb, J., and Hodes, D. (1999) Cytomegalovirus infection and HIV-1 disease progression in infants born to HIV-1–infected women. *N. Eng. J. Med. 341*, 77-84.

(6) Geijtenbeek, T. B., Kwon, D. S., Torensma, R., van Vliet, S. J., van Duijnhoven, G. C., Middel, J., Cornelissen, I. L., Nottet, H. S., KewalRamani, V. N., and Littman, D. R. (2000) DC-SIGN, a dendritic cell–specific HIV-1-binding protein that enhances trans-infection of T cells. *Cell 100*, 587-597.

(7) Cagno, V., Andreozzi, P., D'Alicarnasso, M., Silva, P. J., Mueller, M., Galloux, M., Le Goffic, R., Jones, S. T., Vallino, M., and Hodek, J. (2018) Broad-spectrum non-toxic antiviral nanoparticles with a virucidal inhibition mechanism. *Nat. Mat. 17*, 195-203.

(8) Guo, Y., Feinberg, H., Conroy, E., Mitchell, D. A., Alvarez, R., Blixt, O., Taylor, M. E., Weis, W. I., and Drickamer, K. (2004) Structural basis for distinct ligand-binding and targeting properties of the receptors DC-SIGN and DC-SIGNR. *Nat. Struct. Mol. Biol. 11*, 591-598.

(9) Halary, F., Amara, A., Lortat-Jacob, H., Messerle, M., Delaunay, T., Houlès, C., Fieschi, F., Arenzana-Seisdedos, F., Moreau, J.-F., and Déchanet-Merville, J. (2002) Human cytomegalovirus binding to DC-SIGN is required for dendritic cell infection and target cell trans-infection. *Immun. 17*, 653-664.

(10) Lasala, F., Arce, E., Otero, J. R., Rojo, J., and Delgado, R. (2003) Mannosyl glycodendritic structure inhibits DC-SIGN-mediated Ebola virus infection in cis and in trans. *Antimicrob. Agents Chemother. 47*, 3970-3972.

(11) Liu, P., Ridilla, M., Patel, P., Betts, L., Gallichotte, E., Shahidi, L., Thompson, N. L., and Jacobson, K. (2017) Beyond attachment: Roles of DC-SIGN in dengue virus infection. *Traffic 18*, 218-231.

(12) Maeda, N., Nigou, J., Herrmann, J.-L., Jackson, M., Amara, A., Lagrange, P. H., Puzo, G., Gicquel, B., and Neyrolles, O. (2003) The Cell Surface Receptor DC-SIGN Discriminates between Mycobacterium Species through Selective Recognition of the Mannose Caps on Lipoarabinomannan. *J. Biol. Chem. 278*, 5513-5516.

(13) Garg, R., Trudel, N., and Tremblay, M. J. (2007) Consequences of the natural propensity of Leishmania and HIV-1 to target dendritic cells. *TRENDS Parasito. 23*, 317-324.

(14) Avota, E., Gulbins, E., and Schneider-Schaulies, S. (2011) DC-SIGN mediated sphingomyelinase-activation and ceramide generation is essential for enhancement of viral uptake in dendritic cells. *PLoS Pathog. 7*, e1001290.

(15) Zhang, Q., Su, L., Collins, J., Chen, G., Wallis, R., Mitchell, D. A., Haddleton, D. M., and Becer, C. R. (2014) Dendritic cell lectin-targeting sentinel-like unimolecular glycoconjugates to release an anti-HIV drug. *J. Am. Chem. Soc. 136*, 4325-4332.

(16) Soltero-Higgin, M., Carlson, E. E., Phillips, J. H., and Kiessling, L. L. J. J. o. t. A. C. S. (2004) Identification of inhibitors for UDP-galactopyranose mutase. *J. Am. Chem. Soc. 126*, 10532-10533.

(17) Compain, P., Martin, O. R. J. B., and chemistry, m. (2001) Carbohydrate mimetics-based glycosyltransferase inhibitors. *Bioorg. Med. Chem. 9*, 3077-3092.

(18) Maibaum, J., Liao, S.-M., Vulpetti, A., Ostermann, N., Randl, S., Rüdisser, S., Lorthiois, E., Erbel, P., Kinzel, B., and Kolb, F. A. J. N. c. b. (2016) Small-molecule factor D inhibitors targeting the alternative complement pathway. *Nat. Chem. Biol. 12*, 1105-1115.

(19) Bernardi, A., and Cheshev, P. J. C. A. E. J. (2008) Interfering with the sugar code: design and synthesis of oligosaccharide mimics. *Chem. A. Eur. J. 14*, 7434-7441.

(20) Borrok, M. J., and Kiessling, L. L. J. J. o. t. A. C. S. (2007) Non-carbohydrate inhibitors of the lectin DC-SIGN. *J. Am. Chem. Soc. 129*, 12780-12785.

(21) Mangold, S. L., Prost, L. R., and Kiessling, L. L. J. C. s. (2012) Quinoxalinone inhibitors of the lectin DC-SIGN. *Chem. Sci. 3*, 772-777.

(22) Thépaut, M., Guzzi, C., Sutkeviciute, I., Sattin, S., Ribeiro-Viana, R., Varga, N., Chabrol, E., Rojo, J., Bernardi, A., and Angulo, J. (2013) Structure of a glycomimetic ligand in the carbohydrate recognition domain of C-type lectin DC-SIGN. Structural requirements for selectivity and ligand design. *J. Am. Chem. Soc. 135*, 2518-2529.

(23) Wamhoff, E.-C., Hanske, J., Schnirch, L., Aretz, J., Grube, M., Varón Silva, D., and Rademacher, C. J. A. c. b. (2016) 19F NMR-guided design of glycomimetic Langerin ligands. *ACS Chem. Biol. 11*, 2407-2413.
(24) Ernst, B., and Magnani, J. L. J. N. r. D. d. (2009) From carbohydrate leads to glycomimetic drugs. *Nat. Rev. Drug. Discov. 8*, 661.
(25) Garber, N., Guempel, U., Gilboa-Garber, N., and Royle, R. (1987) Specificity of the fucose-binding lectin of *Pseudomonas aeruginosa. FEMS Microbiol. Lett. 48*, 331-334.
(26) Imberty, A., Wimmerová, M., Mitchell, E. P., and Gilboa-Garber, N. (2004) Structures of the lectins from *Pseudomonas aeruginosa*: insights into the molecular basis for host glycan recognition. *Microb. Infect. 6*, 221-228.
(27) Mitchell, D. A., Fadden, A. J., and Drickamer, K. (2001) A novel mechanism of carbohydrate recognition by the C-type lectins DC-SIGN and DC-SIGNR subunit organization and binding to multivalent ligands. *J. Biol. Chem. 276*, 28939-28945.
(28) Reina, J. J., and Rojo, J. (2013) Glycodendritic structures: tools to interact with DC-SIGN. *Brazil. J. Pharm. Sci. 49*, 109-124.
(29) Dennis, J. W., and Brewer, C. F. (2013) Density dependent lectin-glycan interactions as a paradigm for conditional regulation by post translational modifications. *Mol. Cell. Proteomics*, mcp. R112. 026989.
(30) Becer, C. R., Gibson, M. I., Geng, J., Ilyas, R., Wallis, R., Mitchell, D. A., and Haddleton, D. M. (2010) High-affinity glycopolymer binding to human DC-SIGN and disruption of DC-SIGN interactions with HIV envelope glycoprotein. *J. Am. Chem. Soc. 132*, 15130-15132.
(31) Adams, E. W., Ratner, D. M., Seeberger, P. H., and Hacohen, N. (2008) Carbohydrate-Mediated Targeting of Antigen to Dendritic Cells Leads to Enhanced Presentation of Antigen to T Cells. *Chem. Bio. Chem. 9*, 294-303.
(32) Wang, J., Li, H., Zou, G., and Wang, L.-X. (2007) Novel template-assembled oligosaccharide clusters as epitope mimics for HIV-neutralizing antibody 2G12. Design, synthesis, and antibody binding study. *Org. Biomol. Chem. 5*, 1529-1540.
(33) Wang, S.-K., Liang, P.-H., Astronomo, R. D., Hsu, T.-L., Hsieh, S.-L., Burton, D. R., and Wong, C.-H. (2008) Targeting the carbohydrates on HIV-1: Interaction of oligomannose dendrons with human monoclonal antibody 2G12 and DC-SIGN. *Proc. Natl. Acad. Sci. 105*, 3690-3695.
(34) Tabarani, G., Reina, J. J., Ebel, C., Vivès, C., Lortat-Jacob, H., Rojo, J., and Fieschi, F. (2006) Mannose hyperbranched dendritic polymers interact with clustered organization of DC-SIGN and inhibit gp120 binding. *FEBS Lett. 580*, 2402-2408.
(35) Martínez-Ávila, O., Hijazi, K., Marradi, M., Clavel, C., Campion, C., Kelly, C., and Penadés, S. (2009) Gold manno-glyconanoparticles: Multivalent systems to block HIV-1 gp120 binding to the lectin DC-SIGN. *Chem. Eur. J. 15*, 9874-9888.
(36) Illescas, B. M., Rojo, J., Delgado, R., and Martín, N. (2017) Multivalent glycosylated nanostructures to inhibit Ebola virus infection. *J. Am. Chem. Soc. 139*, 6018-6025.
(37) Rodriguez-Pérez, L., Ramos-Soriano, J., Pérez-Sánchez, A., Illescas, B. M., Muñoz, A., Luczkowiak, J., Lasala, F., Rojo, J., Delgado, R., and Martín, N. (2018) Nanocarbon-based Glycoconjugates as Multivalent Inhibitors of Ebola Virus Infection. *J. Am. Chem. Soc. 140*, 9891-9898.
(38) Kumar, R., Lee, Y. O., Bhalla, V., Kumar, M., and Kim, J. S. (2014) Recent developments of thiacalixarene based molecular motifs. *Chem. Soc. Rev. 43*, 4824-4870.
(39) Taouai, M., Abidi, R., Garcia, J., Siriwardena, A., and Benazza, M. (2014) Synthesis of Unsymmetrical Thioethers Using an Uncommon Base-Triggered 1, 5-Thiol Transfer Reaction of 1-Bromo-2-alkylthiolcarbonates. *J. Org. Chem. 79*, 10743-10751.
(40) Ryu, E.-H., and Zhao, Y. (2005) Efficient synthesis of water-soluble calixarenes using click chemistry. *Org. Lett. 7*, 1035-1037.
(41) Iki, N., Fujimoto, T., and Miyano, S. (1998) A new water-soluble host molecule derived from thiacalixarene. *Chem. Lett. 27*, 625-626.

(42) Morbioli, I., Porkolab, V., Magini, A., Casnati, A., Fieschi, F., and Sansone, F. (2017) Mannosylcalix [n] arenes as multivalent ligands for DC-SIGN. *Carbohydr. Res. 453*, 36-43.
(43) Roy, R., and Kim, J. M. (1999) Amphiphilic p-tert-butylcalix [4] arene scaffolds containing exposed carbohydrate dendrons. *Angew. Chem. Int. Ed. 38*, 369-372.
(44) Weinberg, E. D. (2009) Iron availability and infection. *Biochim. Biophys. Acta (BBA)-General Subjects 1790*, 600-605.
(45) Tabarani, G., Thépaut, M., Stroebel, D., Ebel, C., Vivès, C., Vachette, P., Durand, D., and Fieschi, F. (2009) DC-SIGN neck domain is a pH-sensor controlling oligomerization SAXS and hydrodynamic studies of extracellular domain. *J. Biol. Chem. 284*, 21229-21240.
(46) Feinberg, H., Taylor, M. E., Razi, N., McBride, R., Knirel, Y. A., Graham, S. A., Drickamer, K., and Weis, W. I. (2011) Structural basis for langerin recognition of diverse pathogen and mammalian glycans through a single binding site. *J. Mol. Biol. 405*, 1027-1039.
(47) Geng, J., Mantovani, G., Tao, L., Nicolas, J., Chen, G., Wallis, R., Mitchell, D. A., Johnson, B. R., Evans, S. D., and Haddleton, D. M. (2007) Site-directed conjugation of "clicked" glycopolymers to form glycoprotein mimics: binding to mammalian lectin and induction of immunological function. *J. Am. Chem. Soc. 129*, 15156-15163.
(48) Gringhuis, S. I., Kaptein, T. M., Wevers, B. A., Mesman, A. W., and Geijtenbeek, T. B. (2014) Fucose-specific DC-SIGN signalling directs T helper cell type-2 responses via IKKε-and CYLD-dependent Bcl3 activation. *Nat. Commun. 5*, 3898.
(49) Ordanini, S., Varga, N., Porkolab, V., Thépaut, M., Belvisi, L., Bertaglia, A., Palmioli, A., Berzi, A., Trabattoni, D., and Clerici, M. (2015) Designing nanomolar antagonists of DC-SIGN-mediated HIV infection: ligand presentation using molecular rods. *Chem. Commun. 51*, 3816-3819.
(50) Liu, L., Huang, K., and Yan, C. G. (2010) Syntheses, reactions and crystal structures of 1, 3-alternate p-tert-butylthiacalix [4] arene esters and amides. *J. Incl. Phenom. Macrocycl. Chem. 66*, 349-355.
(51) Alvim, H. G., da Silva Junior, E. N., and Neto, B. A. (2014) What do we know about multicomponent reactions? Mechanisms and trends for the Biginelli, Hantzsch, Mannich, Passerini and Ugi MCRs. *Rsc Adv. 4*, 54282-54299.
(52) Sui, Q., Borchardt, D., and Rabenstein, D. L. (2007) Kinetics and equilibria of cis/trans isomerization of backbone amide bonds in peptoids. *J. Am. Chem. Soc. 129*, 12042-12048.
(53) Taouai, M., Chakroun, K., Vallin-Butruille, A., Cézard, C., and Romdhani, M. (2018) New synthesis of heteroglycoclusters from *p*-tButylcalix[4]arene tetraalkoxyheterohalides as key intermediates. *Org. Chem.*, 186-200.
(54) Timpano, G., Tabarani, G., Anderluh, M., Invernizzi, D., Vasile, F., Potenza, D., Nieto, P. M., Rojo, J., Fieschi, F., and Bernardi, A. (2008) Synthesis of Novel DC-SIGN Ligands with an α-Fucosylamide Anchor. *Chem. Bio. Chem. 9*, 1921-1930.
(55) Cattiaux, L., Porkolab, V., Fieschi, F., and Mallet, J.-M. (2018) New branched amino acids for high affinity dendrimeric DC-SIGN ligands. *Bioorg. Med. Chem. 26*, 1006-1015.
(56) Bertolotti, B., Sutkeviciute, I., Ambrosini, M., Ribeiro-Viana, R., Rojo, J., Fieschi, F., Dvořáková, H., Kašáková, M., Parkan, K., and Hlaváčková, M. (2017) Polyvalent C-glycomimetics based on L-fucose or D-mannose as potent DC-SIGN antagonists. *Org. Biomol. Chem. 15*, 3995-4004.
(57) Luczkowiak, J., Sattin, S., Sutkeviciute, I., Reina, J. J., Sánchez-Navarro, M., Thépaut, M., Martínez-Prats, L., Daghetti, A., Fieschi, F., and Delgado, R. (2011) Pseudosaccharide functionalized dendrimers as potent inhibitors of DC-SIGN dependent Ebola pseudotyped viral infection. *Bioconjug. Chem. 22*, 1354-1365.
(58) Varga, N., Sutkeviciute, I., Ribeiro-Viana, R., Berzi, A., Ramdasi, R., Daghetti, A., Vettoretti, G., Amara, A., Clerici, M., and Rojo, J. (2014) A multivalent inhibitor of the DC-SIGN dependent uptake of HIV-1 and Dengue virus. *Biomat. 35*, 4175-4184.

(59) Puchhammer-Stöckl, E., Görzer, I., Zoufaly, A., Jaksch, P., Bauer, C. C., Klepetko, W., and Popow-Kraupp, T. (2006) Emergence of multiple cytomegalovirus strains in blood and lung of lung transplant recipients. *Transplant. 81*, 187-194.
(60) Crowe, W. E., Maglova, L. M., Ponka, P., and Russell, J. M. (2004) Human cytomegalovirus-induced host cell enlargement is iron dependent. *Am. J. Physiol. -Cell Physiol. 287*, C1023-C1030.
(61) Vanarsdall, A. L., and Johnson, D. C. (2012) Human cytomegalovirus entry into cells. *Curr. Opin. Virol. 2*.
(62) Chéneau, C., Coulon, F., Porkolab, V., Fieschi, F., Laurant, S., Razanajaona-Doll, D., Pin, J.-J., Borst, E. M., Messerle, M., and Bressollette-Bodin, C. (2018) Fine Mapping the Interaction Between Dendritic Cell-Specific Intercellular Adhesion Molecule (ICAM)-3-Grabbing Nonintegrin and the Cytomegalovirus Envelope Glycoprotein B. *J. Infect. Dis.*, jiy194.
(63) Baldwin, J., Maus, E., Zanotti, B., Volin, M. V., Tandon, R., Shukla, D., and Tiwari, V. (2015) A role for 3-O-sulfated heparan sulfate in promoting human cytomegalovirus infection in human iris cells. *J. Virol. 89*, 5185-5192.
(64) Burke, H. G., and Heldwein, E. E. (2015) Crystal structure of the human cytomegalovirus glycoprotein B. *PLoS Pathog. 11*, e1005227.
(65) Brument, S., Cheneau, C., Brissonnet, Y., Deniaud, D., Halary, F., and Gouin, S. (2017) Polymeric mannosides prevent DC-SIGN-mediated cell-infection by cytomegalovirus. *Org. Biomol. Chem. 15*, 7660-7671.
(66) Rhein, B. A., and Maury, W. J. J. C. c. m. r. (2015) Ebola virus entry into host cells: Identifying therapeutic strategies. *Curr. Clin. Micro. Rpt. 2*, 115-124.
(67) Wool-Lewis, R. J., and Bates, P. J. J. o. v. (1998) Characterization of Ebola virus entry by using pseudotyped viruses: identification of receptor-deficient cell lines. *J. Virol. 72*, 3155-3160.
(68) Henao-Restrepo, A. M., Camacho, A., Longini, I. M., Watson, C. H., Edmunds, W. J., Egger, M., Carroll, M. W., Dean, N. E., Diatta, I., and Doumbia, M. (2017) Efficacy and effectiveness of an rVSV-vectored vaccine in preventing Ebola virus disease: final results from the Guinea ring vaccination, open-label, cluster-randomised trial (Ebola Ça Suffit!). *Lancet 389*, 505-518.
(69) Uyeki, T., Mehta, A., Davey Jr, R., Liddell, A., Wolf, T., Vetter, P., Schmiedel, S., Grunewald, T., Jacobs, M., and Arribas, J. (2016) Working Group of the USECNoCMoEVDPitUS. *Eur.* 636-646.
(70) Yazdanpanah, Y., Arribas, J. R., and Malvy, D. (2015) Treatment of Ebola virus disease. *Intens. Care Med. 41*, 115-117.
(71) Nyakatura, E. K., Frei, J. C., and Lai, J. R. (2014) Chemical and structural aspects of Ebola virus entry inhibitors. *ACS Infect. dis. 1*, 42-52.
(72) Baize, S., Pannetier, D., Oestereich, L., Rieger, T., Koivogui, L., Magassouba, N. F., Soropogui, B., Sow, M. S., Keïta, S., and De Clerck, H. (2014) Emergence of Zaire Ebola virus disease in Guinea. *N. Eng. J. Med. 371*, 1418-1425.
(73) Davey, R. T., Jr., Dodd, L., Proschan, M. A., Neaton, J., Neuhaus Nordwall, J., Koopmeiners, J. S., Beigel, J., Tierney, J., Lane, H. C., Fauci, A. S., et al (2016) A Randomized, Controlled Trial of ZMapp for Ebola Virus Infection. *N. Engl. J. Med. 375*, 1448-1456.
(74) Warren, T. K., Jordan, R., Lo, M. K., Ray, A. S., Mackman, R. L., Soloveva, V., Siegel, D., Perron, M., Bannister, R., and Hui, H. C. (2016) Therapeutic efficacy of the small molecule GS-5734 against Ebola virus in rhesus monkeys. *Nat. 531*, 381.
(75) Taylor, R., Kotian, P., Warren, T., Panchal, R., Bavari, S., Julander, J., Dobo, S., Rose, A., El-Kattan, Y., and Taubenheim, B. (2016) BCX4430–a broad-spectrum antiviral adenosine nucleoside analog under development for the treatment of Ebola virus disease. *J. Infect. Public health 9*, 220-226.
(76) Lasala, F., Arce, E., Otero, J. R., Rojo, J., and Delgado, R. (2003) Mannosyl glycodendritic structure inhibits DC-SIGN-mediated Ebola virus infection in cis and in trans. *Antimicrob. Agents Chemother. 47*, 3970-3972.

(77) Alvarez, C. P., Lasala, F., Carrillo, J., Muñiz, O., Corbí, A. L., and Delgado, R. (2002) C-type lectins DC-SIGN and L-SIGN mediate cellular entry by Ebola virus in cis and in trans. *J. Virol. 76*, 6841-6844.

(78) Connor, R. I., Chen, B. K., Choe, S., and Landau, N. R. (1995) Vpr is required for efficient replication of human immunodeficiency virus type-1 in mononuclear phagocytes. *Virol. 206*, 935-944.

(79) Yang, S., Delgado, R., Barker, C. S., Yang, Z.-Y., Nabel, G. J., King, S. R., Woffendin, C., Xu, L., and Nolan, G. P. (1999) Generation of retroviral vector for clinical studies using transient transfection. *Hum. Gene Ther. 10*, 123-132.